

Randomized Midpoint Method for Log-Concave Sampling under Constraints

Yifeng Yu^{*} Lu Yu[†]

May 27, 2025

Abstract

In this paper, we study the problem of sampling from log-concave distributions supported on convex, compact sets, with a particular focus on the randomized midpoint discretization of both vanilla and kinetic Langevin diffusions in this constrained setting. We propose a unified proximal framework for handling constraints via a broad class of projection operators, including Euclidean, Bregman, and Gauge projections. Within this framework, we establish non-asymptotic bounds in both \mathcal{W}_1 and \mathcal{W}_2 distances, providing precise complexity guarantees and performance comparisons. In addition, our analysis leads to sharper convergence guarantees for both vanilla and kinetic Langevin Monte Carlo under constraints, improving upon existing theoretical results.

1 Introduction

Sampling from probability distributions plays a critical role in various fields of science and engineering, especially when dealing with convex and compact sets [ADFDJ03, GCSR95, Stu10]. In this context, the problem involves sampling from a probability measure ν on such sets, characterized by its density function

$$\nu(\boldsymbol{\theta}) = \frac{e^{-U(\boldsymbol{\theta})}}{\int_{\mathbb{R}^p} e^{-U(\boldsymbol{\theta})} d\boldsymbol{\theta}},$$

Here, $U(\boldsymbol{\theta}) = f(\boldsymbol{\theta}) + \ell_{\mathcal{K}}(\boldsymbol{\theta})$, where $f(\boldsymbol{\theta})$ represents a potential function and $\ell_{\mathcal{K}}(\boldsymbol{\theta})$ is an indicator function ensuring $\boldsymbol{\theta}$ lies within the convex and compact set $\mathcal{K} \subset \mathbb{R}^p$

$$\ell_{\mathcal{K}}(\boldsymbol{\theta}) := \begin{cases} +\infty & \text{if } \boldsymbol{\theta} \notin \mathcal{K} \\ 0 & \text{if } \boldsymbol{\theta} \in \mathcal{K}. \end{cases}$$

Solving this constrained sampling problem is challenging and has garnered considerable interest across various fields, including computer science and statistics. In the realm of computer science, a line of research initiated by [DFK91] explored polynomial-time algorithms for uniformly sampling convex bodies. This has been followed by seminal studies on the convergence properties of the Ball Walk and the Hit-and-Run algorithm toward uniform density on a convex body or, more broadly, to log-concave densities [KLS97, KVZ24, Lov99, LS93, LV07, Smi84]. Another category of samplers addresses the geometric structure of convex constraints, including Riemannian Hamiltonian Monte

^{*}Department of Mathematical Sciences, Tsinghua University yyf22@mails.tsinghua.edu.cn

[†]Department of Data Science, City University of Hong Kong lu.yu@cityu.edu.hk

Carlo [BSU12, KLSV22], Gibbs sampling [GSL92], and Mirror Langevin methods [AC21, CLGL⁺20, HKRC18, ZPFP20].

In recent years, leveraging optimization techniques to facilitate sampling has become a prevalent approach. By formulating the sampling challenge as an optimization problem, methods like projected stochastic gradient descent [BEL15, BEL18, Lam21, Leh23], penalty method [GHZ24], proximal approaches [BDMP17, DMP18, SR20, CKJK24], particle-based algorithms [LLK⁺22], and mirror descent [AC21, CLGL⁺20, HKRC18, ZPFP20] have proven effective in navigating the target distribution to generate samples. Advances in deep learning and generative modeling, such as generative adversarial networks [GPAM⁺14] and variational autoencoders [KW13], have led to powerful sampling methods for complex, high-dimensional distributions, including those defined on a convex body [OHHTD22]. Among these works, [BDMP17, GHZ24] are the most closely aligned with the spirit of this study. We highlight the most relevant findings from both studies alongside our main results. A detailed comparison and discussion are provided in Appendix A.

In the absence of constraints, a wide range of diffusion-based samplers have been developed, leveraging discretizations of Itô diffusions to efficiently approximate the target distribution. A canonical example is Langevin Monte Carlo (LMC) [Dal17, DM17, EH21, EHZ22, EMS18, MFWB22, MHFH⁺23, RRT17, RT96], a Markov chain Monte Carlo method that simulates the motion of a particle in a potential defined by the target density. It corresponds to the Euler-Maruyama discretization of the Langevin diffusion. A popular extension, kinetic Langevin Monte Carlo (KLMC), discretizes the kinetic Langevin diffusion, which incorporates momentum and friction to balance exploration and exploitation [Ein05, VS06]. As shown by [Nel67], the Langevin diffusion is a rescaled limit of the kinetic version. Theoretical properties such as ergodicity and mixing time have been studied in works like [DRD20, EGZ19]. To improve discretization accuracy, [SL19] propose the randomized midpoint scheme for KLMC (RKLMC), showing its advantages in error tolerance and condition number dependence. Subsequent work further analyzed its probabilistic properties [HBE20, YKD23], its suitability for parallel implementation [YD24], and its performance and acceleration benefits in generative modeling [GCC24, LJ24, YY25]. However, the behavior of the midpoint randomization method for (kinetic) Langevin Monte Carlo under constrained settings remains unexplored. Additionally, this method, along with the previously studied LMC and KLMC algorithms, relies on the smoothness of the target density, which is violated in the constrained settings considered here.

In this work, we focus on the randomized midpoint discretization of both vanilla and kinetic Langevin diffusions in constrained settings. To address the non-smoothness of the target density ν , we adopt a regularization technique based on projecting onto \mathcal{K} , effectively reducing the constrained problem to an unconstrained one. Our framework supports various projections, including metric-based projections such as the Euclidean projection, which corresponds to the Moreau envelope of the indicator function $\ell_{\mathcal{K}}$ [BDMP17, DMP18, Per16, RW09]; more generally, the Bregman projection, widely used in clustering, classification, and outliers detection [Gho19, XNZ08, XJRN02]; and scaling-based projections, such as the Gauge projection [LBGH22, Mha22], which can be efficiently performed via a membership oracle [Mha22]. The resulting smooth surrogate density closely approximates the target density. We then apply the unconstrained randomized midpoint scheme to both vanilla and kinetic Langevin diffusions for sampling from the surrogate distribution, resulting in CRLMC and CRKLMC algorithms, respectively. A key contribution of our work is the first derivation of a lower bound on the Wasserstein distance between the surrogate and the target, complementing existing upper bounds. Our sharper approximation analysis for the proposed surrogate density also yields improved error bounds for the constrained LMC and KLMC algorithms (referred to as CLMC and CKLMC in this work), originally introduced in [BDMP17, GHZ24]. Table 1 summarizes all of our iteration complexity results, along with existing results for comparison.

Our main contributions are as follows.

- In Section 2.1, we demonstrate that our proposed framework can incorporate various projection options, such as Euclidean, Bregman, and Gauge projections. Notably, the latter two have received limited attention in the context of constrained sampling.
- In Section 2.2, we analyze the approximation error between the proposed surrogate density and the target in terms of the Wasserstein- q ($q \geq 1$) distance, and establish both upper bounds and partially matching lower bounds. Our novel proof is based on optimal transport theory and exploits radial alignment in polar coordinates to tightly control the Wasserstein distance between ν^λ and ν . To the best of our knowledge, the derivation of such lower bounds has not been addressed in prior work.
- In Section 2.3 and Section 2.4, we introduce the CRLMC and CRKLMC algorithms and provide convergence analyses under both Wasserstein-1 and Wasserstein-2 distances.
- In Section 2.5, we revisit the CLMC and CKLMC algorithms. Building on our refined analysis of the approximation error between ν^λ and ν , we derive sharper non-asymptotic guarantees on their sampling error, improving upon existing results.

Notation. Denote the p -dimensional Euclidean space by \mathbb{R}^p . We use $\boldsymbol{\theta}$ for deterministic vectors and $\boldsymbol{\vartheta}$ for random vectors. \mathbf{I}_p and $\mathbf{0}_p$ denote the $p \times p$ identity and zero matrices, respectively. For symmetric matrices \mathbf{A} and \mathbf{B} , we write $\mathbf{A} \preceq \mathbf{B}$ (or $\mathbf{B} \succeq \mathbf{A}$) if $\mathbf{B} - \mathbf{A}$ is positive semi-definite. The gradient and Hessian of a function f are denoted by ∇f and $\nabla^2 f$, respectively. Given probability measures μ and ν on $(\mathbb{R}^p, \mathcal{B}(\mathbb{R}^p))$, the Wasserstein- q distance is defined as $W_q(\mu, \nu) = (\inf_{\varrho \in \Gamma(\mu, \nu)} \int_{\mathbb{R}^p \times \mathbb{R}^p} \|\boldsymbol{\theta} - \boldsymbol{\theta}'\|_2^q d\varrho(\boldsymbol{\theta}, \boldsymbol{\theta}'))^{1/q}$, where the infimum is over all couplings ϱ with marginals μ and ν .

2 Main Results

We begin by introducing a smooth approximation of the target density and deriving Wasserstein bounds on its distance to the target.

2.1 Smooth Approximation for the Target Density

The absence of smoothness in the target distribution ν presents significant challenges because sampling algorithms often depend on the smoothness properties of the target distribution to effectively explore the space and produce representative samples. Motivated by this, we consider the approximation for $\ell_{\mathcal{K}}$ of the form

$$\ell_{\mathcal{K}}^\lambda(\boldsymbol{\theta}) := \frac{1}{2\lambda^2} d_{\mathcal{K}}(\boldsymbol{\theta}),$$

where $\lambda > 0$ is the tuning parameter and $d_{\mathcal{K}} : \mathbb{R}^p \rightarrow \mathbb{R}_+$ is a distance function that quantifies the distance between $\boldsymbol{\theta}$ and the constraint set \mathcal{K} . We will later introduce specific choices for $d_{\mathcal{K}}$. Define

$$U^\lambda(\boldsymbol{\theta}) := f(\boldsymbol{\theta}) + \ell_{\mathcal{K}}^\lambda(\boldsymbol{\theta}),$$

and the corresponding surrogate target density ν^λ

$$\nu^\lambda(\boldsymbol{\theta}) := \frac{e^{-U^\lambda(\boldsymbol{\theta})}}{\int_{\mathbb{R}^p} e^{-U^\lambda(\boldsymbol{\theta}')} d\boldsymbol{\theta}'}.$$

We assume the convex and compact set \mathcal{K} satisfies the following assumption.

Table 1: Iteration complexities of {CL, CKL, CRL, CRKL}MC algorithms for achieving ε -accuracy in W_1 and W_2 distances under different projection operators (with Euclidean projection as a special case of Bregman projection). This table also includes existing results for CLMC (also known as MYULA [BDMP17] and PSGLD [GHZ24]) and CKLMC (also referred to as PSGULMC [GHZ24]). For methods involving both distances, the complexities are listed in separate rows.

Algorithm	Projection	Metric	Complexity
MYULA in [BDMP17]	Euclidean	W_1	$\tilde{\mathcal{O}}(\varepsilon^{-6})$
PSGLD in [GHZ24]	Euclidean	W_2	$\tilde{\mathcal{O}}(\varepsilon^{-18})$
CLMC (Theorem 5)	Bregman, Gauge	W_1	$\tilde{\mathcal{O}}(\varepsilon^{-4})$
		W_2	$\tilde{\mathcal{O}}(\varepsilon^{-6+4/p})$
PSGULMC in [GHZ24]	Euclidean	W_2	$\tilde{\mathcal{O}}(\varepsilon^{-13})$
CKLMC (Theorem 6)	Bregman, Gauge	W_1	$\tilde{\mathcal{O}}(\varepsilon^{-4})$
		W_2	$\tilde{\mathcal{O}}(\varepsilon^{-7+6/p})$
CRLMC (Theorem 3)	Bregman, Gauge	W_1	$\tilde{\mathcal{O}}(\varepsilon^{-10/3})$
		W_2	$\tilde{\mathcal{O}}(\varepsilon^{-6+16/(3p)})$
CRKLMC (Theorem 4)	Bregman, Gauge	W_1	$\tilde{\mathcal{O}}(\varepsilon^{-8/3})$
		W_2	$\tilde{\mathcal{O}}(\varepsilon^{-5+14/(3p)})$

Assumption 1. Given constants $0 < r < R < \infty$, it holds that $\mathcal{B}_2(r) \subset \mathcal{K} \subset \mathcal{B}_2(R)$, where $\mathcal{B}_2(r)$ denotes the Euclidean ball of radius r centered at the origin.

This assumption has been made in the work of constrained sampling [BEL18, BDMP17, GHZ24, Lam21]. For clarity of presentation, we assume in Assumption 1 that the origin $\mathbf{0} \in \mathcal{K}$, though our results remain valid without this condition. We also assume the potential function f satisfies the following.

Assumption 2. The function $f : \mathbb{R}^p \rightarrow \mathbb{R}$ is lower bounded on \mathbb{R}^p .

Furthermore, we require the distance function $d_{\mathcal{K}}$ to satisfy the following assumption.

Assumption 3. There exists some constants $0 < c_1 \leq c_2$ such that $c_1 \|\boldsymbol{\theta} - \mathbf{P}_{\mathcal{K}}(\boldsymbol{\theta})\|_2^2 \leq d_{\mathcal{K}}(\boldsymbol{\theta}) \leq c_2 \|\boldsymbol{\theta} - \mathbf{P}_{\mathcal{K}}(\boldsymbol{\theta})\|_2^2$, where $\mathbf{P}_{\mathcal{K}} : \mathbb{R}^p \rightarrow \mathbb{R}^p$ is a projection operator onto set \mathcal{K} . Moreover, $d_{\mathcal{K}}(\boldsymbol{\theta}) \geq 0$ for all $\boldsymbol{\theta} \in \mathbb{R}^p$, and $d_{\mathcal{K}}(\boldsymbol{\theta}) = 0$ whenever $\boldsymbol{\theta} \in \mathcal{K}$.

This property of $d_{\mathcal{K}}$ ensures U^λ inherits smoothness and strong convexity from f . Below, we present two types of approximations for $\ell_{\mathcal{K}}$, based on commonly used projection classes: **metric-based** and **scaling-based**, both satisfying Assumption 3 and effectively approximating the indicator function.

Example 2.1. [Metric-based Projection] Consider the Bregman Projection $\mathbf{P}_{\mathcal{K}}^B : \mathbb{R}^p \rightarrow \mathcal{K}$

$$\mathbf{P}_{\mathcal{K}}^B(\boldsymbol{\theta}) := \operatorname{argmin}_{\boldsymbol{\theta}' \in \mathcal{K}} (\boldsymbol{\theta} - \boldsymbol{\theta}')^\top Q (\boldsymbol{\theta} - \boldsymbol{\theta}')$$

where $Q \in \mathbb{R}^{d \times d}$ is a positive semi-definite symmetric matrix.

Note that the Bregman divergence $D_F(\boldsymbol{\theta}, \boldsymbol{\theta}') := (\boldsymbol{\theta} - \boldsymbol{\theta}')^\top Q(\boldsymbol{\theta} - \boldsymbol{\theta}')$ is the squared Mahalanobis distance, generated by function $F(\boldsymbol{\theta}) := \frac{1}{2}\boldsymbol{\theta}^\top Q\boldsymbol{\theta}$. In this case, we consider the distance function of the form

$$d_{\mathcal{K}}(\boldsymbol{\theta}) = \|\boldsymbol{\theta} - \mathbb{P}_{\mathcal{K}}^B(\boldsymbol{\theta})\|_2^2. \quad (2.1)$$

Therefore, the Bregman projection induces the following approximation to $\ell_{\mathcal{K}}$

$$\ell_{\mathcal{K}}^{B,\lambda}(\boldsymbol{\theta}) = \frac{1}{2\lambda^2} \|\boldsymbol{\theta} - \mathbb{P}_{\mathcal{K}}^B(\boldsymbol{\theta})\|_2^2 = \inf_{\boldsymbol{\theta}' \in \mathbb{R}^p} \left(\ell_{\mathcal{K}}(\boldsymbol{\theta}') + \frac{1}{2\lambda^2} (\boldsymbol{\theta} - \boldsymbol{\theta}')^\top Q(\boldsymbol{\theta} - \boldsymbol{\theta}') \right).$$

and $U^{B,\lambda}(\boldsymbol{\theta}) = f(\boldsymbol{\theta}) + \ell_{\mathcal{K}}^{B,\lambda}(\boldsymbol{\theta})$. When $Q = I$, the Bregman projection recovers the Euclidean projection, which yields the Moreau envelope.

Example 2.2. [Scaling-based projection] The Gauge projection $\mathbb{P}_{\mathcal{K}}^G : \mathbb{R}^p \rightarrow \mathcal{K}$ is defined as

$$\mathbb{P}_{\mathcal{K}}^G(\boldsymbol{\theta}) := \frac{\boldsymbol{\theta}}{g_{\mathcal{K}}(\boldsymbol{\theta})}$$

where $g_{\mathcal{K}} : \mathbb{R}^p \rightarrow \mathbb{R}$ is a variant of the Gauge function (also known as the Minkowski functional) associated with the set \mathcal{K} , given by

$$g_{\mathcal{K}}(\boldsymbol{\theta}) := \inf\{t \geq 1 : \boldsymbol{\theta} \in t\mathcal{K}\}.$$

The function $g_{\mathcal{K}}$ characterizes the scaling required to project $\boldsymbol{\theta}$ onto the set \mathcal{K} . In this case, we consider the distance function as

$$d_{\mathcal{K}}(\boldsymbol{\theta}) = (g_{\mathcal{K}}(\boldsymbol{\theta}) - 1)^2.$$

Unlike the metric-based projection (2.1), which inherits convexity from the Moreau envelope, the Gauge projection is defined within a non-Euclidean geometry. Moreover, under the assumption on \mathcal{K} , the distance function $d_{\mathcal{K}}$ satisfies Assumption 3 with constants $c_1 = 1/R^2$ and $c_2 = 1/r^2$. Set $\ell_{\mathcal{K}}^{G,\lambda}(\boldsymbol{\theta}) = \frac{1}{2\lambda^2}(g_{\mathcal{K}}(\boldsymbol{\theta}) - 1)^2$. The corresponding surrogate function is defined via $U^{G,\lambda}(\boldsymbol{\theta}) := f(\boldsymbol{\theta}) + \ell_{\mathcal{K}}^{G,\lambda}(\boldsymbol{\theta})$.

2.2 Wasserstein Distance Bounds Between Distributions ν^λ and ν

In this section, we establish upper and lower Wasserstein bounds between ν and its approximation ν^λ , demonstrating that the distance vanishes as λ approaches zero.

Proposition 1. Under Assumptions 1-3, for any $q \geq 1$ and when $\lambda = o(r/p)$, it holds that

$$W_q(\nu, \nu^\lambda) = \begin{cases} \mathcal{O}(\lambda), & 1/p + 1/q > 1 \\ \mathcal{O}(\lambda \log^{1/q}(\frac{1}{\lambda})), & 1/p + 1/q = 1 \\ \mathcal{O}(\lambda^{1/p+1/q}), & 1/p + 1/q < 1. \end{cases}$$

This theorem captures a phase transition in $W_q(\nu, \nu^\lambda)$ that depends on the relation between dimension p and Wasserstein order q , exhibiting linear convergence when $1/p + 1/q > 1$, and slower rates in higher dimensions or for higher-order distances. When $q = 1$, our result aligns with the bound $W_1(\nu, \nu^\lambda) = \mathcal{O}(\lambda)$ stated in [BDMP17, Proposition 5]. For $q = 2$, our analysis yields the rate $W_2(\nu, \nu^\lambda) = \mathcal{O}(\lambda^{1/2+1/p})$ when $p > 2$. In comparison, [GHZ24] studies a special case of our Example

2.1 ($Q = I$), obtaining the bound $W_2(\nu, \nu^\lambda) = \mathcal{O}(\lambda^{1/4} \log^{1/8}(1/\lambda^2))$. Thus, our result provides a substantially sharper bound.

Our improved results rely on a novel proof strategy based on optimal transport, where a transport map is constructed to align the radial distributions of ν^λ and ν . This radial alignment enables a sharper and more structured analysis of the Wasserstein distance. A high-level overview of the proof is provided in Appendix B.1.

We also derive the following lower bound on $W_q(\nu^\lambda, \nu)$.

Proposition 2. *Under Assumptions 1–3, for any $q \geq 1$, if*

$$\frac{\int_{\mathcal{K}} \|\boldsymbol{\theta}\|_2^q e^{-U(\boldsymbol{\theta})} d\boldsymbol{\theta}}{\int_{\mathcal{K}} e^{-U(\boldsymbol{\theta})} d\boldsymbol{\theta}} \neq \lim_{\lambda \rightarrow 0} \frac{\int_{\mathcal{K}^c} \|\boldsymbol{\theta}\|_2^q e^{-U^\lambda(\boldsymbol{\theta})} d\boldsymbol{\theta}}{\int_{\mathcal{K}^c} e^{-U^\lambda(\boldsymbol{\theta})} d\boldsymbol{\theta}}, \quad (2.2)$$

and if f and $d_{\mathcal{K}}$ are both smooth, then for a sufficiently small λ , it holds that $W_q(\nu, \nu^\lambda) = \Omega(\lambda)$.

Condition (2.2) states that the conditional q -th moment over \mathcal{K}^c under the surrogate density does not converge to that of the target distribution supported on \mathcal{K} as $\lambda \rightarrow 0$. To our knowledge, this represents the first lower bounds for the Wasserstein distance between the surrogate distribution and the target distribution. Based on the results outlined in the preceding proposition, when $1/p + 1/q > 1$ and with a sufficiently small λ , the lower bound aligns with the rate estimates from Proposition 1 up to a constant factor, thereby confirming the optimality of the upper bound for this case.

2.3 Randomized Midpoint Method for Langevin Diffusion under Constraints

Our goal is to sample from the surrogate density $\nu^\lambda \propto \exp(-U^\lambda)$. Throughout this section, we assume that the potential f is strongly convex and smooth, and $d_{\mathcal{K}}$ is smooth.

Assumption 4. *The distance function $d_{\mathcal{K}}$ is M_0 -smooth for a constant $0 < M_0 < \infty$. Moreover, the function $f : \mathbb{R}^p \rightarrow \mathbb{R}$ is twice differentiable with Hessian satisfying $m \preccurlyeq \nabla^2 f \preccurlyeq M$ for some constants $0 < m \leq M < \infty$.*

Under Assumptions 3 and 4, the surrogate potential U^λ is m -strongly convex and M^λ -smooth with $M^\lambda = M + M_0/\lambda^2$. Together with Assumptions 1 and 2, it follows that $\int_{\mathbb{R}^p} e^{-U^\lambda}(\boldsymbol{\theta}) d\boldsymbol{\theta} < \infty$. In Appendix C, we show that the surrogate potentials given in Example 2.1 and Example 2.2 satisfy these conditions.

These favorable properties enable the application of Langevin Monte Carlo and its variants, originally designed for unconstrained settings, to sample from $\nu^\lambda \propto \exp(-U^\lambda)$. Let $\boldsymbol{\vartheta}_0 \in \mathbb{R}^p$ be a random vector drawn from a distribution ν_0 and let $\mathbf{W} = (\mathbf{W}_t : t \geq 0)$ be a p -dimensional Brownian motion that is independent of $\boldsymbol{\vartheta}_0$. One can sample from the approximate distribution ν^λ using vanilla Langevin diffusion, defined as the strong solution to the stochastic differential equation (SDE)

$$d\mathbf{L}_t^{\text{LD}} = -\nabla U^\lambda(\mathbf{L}_t^{\text{LD}}) dt + \sqrt{2} d\mathbf{W}_t, \quad t \geq 0, \quad \mathbf{L}_0^{\text{LD}} = \boldsymbol{\vartheta}_0. \quad (2.3)$$

This equation has a unique strong solution, which is a continuous-time Markov process, termed Langevin diffusion. Under the further assumptions on the potential U^λ , such as strong convexity, the Langevin diffusion is ergodic, geometrically mixing and has ν^λ as its unique invariant distribution [Bha78]. Moreover, ν^λ can be sampled via a suitable discretization of Langevin diffusion, as

done in the Langevin Monte Carlo algorithm using Euler discretization. Specifically, for a small step size $h > 0$ and $\Delta_h \mathbf{W}_t = \mathbf{W}_{t+h} - \mathbf{W}_t$, the following approximation holds

$$\mathbf{L}_{t+h}^{\text{LD}} = \mathbf{L}_t^{\text{LD}} - \int_0^h \nabla U^\lambda(\mathbf{L}_{t+s}^{\text{LD}}) ds + \sqrt{2} \Delta_h \mathbf{W}_t \approx \mathbf{L}_t^{\text{LD}} - h \nabla U^\lambda(\mathbf{L}_t^{\text{LD}}) + \sqrt{2} \Delta_h \mathbf{W}_t.$$

Motivated by this, [BDMP17, GHZ24] propose to use the Markov chain $(\boldsymbol{\vartheta}_k^{\text{CLMC}})_{k \in \mathbb{N}_+}$, which converges to ν^λ as the step size h goes to zero. Approximating $\boldsymbol{\vartheta}_k^{\text{CLMC}} \approx \mathbf{L}_{kh}^{\text{LD}}$, the update rule is

$$\boldsymbol{\vartheta}_{k+1}^{\text{CLMC}} = \boldsymbol{\vartheta}_k^{\text{CLMC}} - h \nabla U^\lambda(\boldsymbol{\vartheta}_k^{\text{CLMC}}) + \sqrt{2} (\mathbf{W}_{(k+1)h} - \mathbf{W}_{kh}). \quad (2.4)$$

As an alternative to the Euler discretization method for SDE (2.3), we consider the randomized midpoint method introduced in [SL19]. Unlike the Euler method, the randomized midpoint method evaluates the integral $\int_0^h \nabla U^\lambda(\mathbf{L}_{t+s}^{\text{LD}}) ds$ at a random point within the time interval $[0, h]$ rather than at the start. Let ι be a uniform random variable on $[0, 1]$, independent of the Brownian motion \mathbf{W} . The randomized midpoint method exploits the approximation

$$\mathbf{L}_{t+h}^{\text{LD}} = \mathbf{L}_t^{\text{LD}} - \int_0^h \nabla U^\lambda(\mathbf{L}_{t+s}^{\text{LD}}) ds + \sqrt{2} \Delta_h \mathbf{W}_t \approx \mathbf{L}_t^{\text{LD}} - h \nabla U^\lambda(\mathbf{L}_{t+h\iota}^{\text{LD}}) + \sqrt{2} \Delta_h \mathbf{W}_t.$$

The constrained randomized midpoint Langevin Monte Carlo (CRLMC) algorithm is formally defined as follows for each iteration $k = 1, 2, \dots$

- **Step 1** Generate independent $\boldsymbol{\xi}'_k, \boldsymbol{\xi}''_k \sim \mathcal{N}(\mathbf{0}, \mathbf{I}_p)$ and uniform random variable $\iota_k \sim \text{Unif}[0, 1]$.
- **Step 2** Set $\boldsymbol{\xi}_k = \sqrt{\iota_k} \boldsymbol{\xi}'_k + \sqrt{1 - \iota_k} \boldsymbol{\xi}''_k$ and define the $(k+1)$ -th iterate $\boldsymbol{\vartheta}_{k+1}^{\text{CRLMC}}$ by

$$\begin{aligned} \boldsymbol{\vartheta}_{k+\iota}^{\text{CRLMC}} &= \boldsymbol{\vartheta}_k^{\text{CRLMC}} - h \iota_k \nabla U^\lambda(\boldsymbol{\vartheta}_k^{\text{CRLMC}}) + \sqrt{2h\iota_k} \boldsymbol{\xi}'_k \\ \boldsymbol{\vartheta}_{k+1}^{\text{CRLMC}} &= \boldsymbol{\vartheta}_k^{\text{CRLMC}} - h \nabla U^\lambda(\boldsymbol{\vartheta}_{k+\iota}^{\text{CRLMC}}) + \sqrt{2h} \boldsymbol{\xi}_k. \end{aligned}$$

Let ν_n^{CRLMC} denote the distribution of $\boldsymbol{\vartheta}_n^{\text{CRLMC}}$. Combined the analysis of $W_q(\nu_n^{\text{CRLMC}}, \nu^\lambda)$ with that of $W_q(\nu, \nu^\lambda)$ in Section 2.2, the following theorem characterizes the selection of λ , step size h , and iteration count n for CRLMC to achieve a given precision level. Due to space limitations, we present only the key factors in the convergence rates here; detailed proofs with explicit constants and parameter dependencies are provided in the appendix.

Theorem 3. *Under Assumptions 1-4, let the target precision level $\varepsilon \in (0, 1)$ be small, and set the initial point $\boldsymbol{\vartheta}_0^{\text{CRLMC}}$ to be the minimizer of the function f .*

(a) *Set $\lambda = \Theta(h^{3p/(9p+2)})$, and choose step size $h > 0$ and $n \in \mathbb{N}_+$ so that*

$$h = \mathcal{O}\left(\varepsilon^{\frac{18p+4}{3p+6}}\right) \quad \text{and} \quad n = \tilde{\Omega}\left(\varepsilon^{-\frac{18p+4}{3p+6}}\right)$$

then we have $W_2(\nu_n^{\text{CRLMC}}) = \tilde{\mathcal{O}}(\varepsilon)$.

(b) *Set $\lambda = \Theta(h^{3/10})$, and choose $h > 0$ and $n \in \mathbb{N}_+$ so that*

$$h = \mathcal{O}\left(\varepsilon^{\frac{10}{3}}\right) \quad \text{and} \quad n = \tilde{\Omega}\left(\varepsilon^{-\frac{10}{3}}\right).$$

then we have $W_1(\nu_n^{\text{CRLMC}}) = \tilde{\mathcal{O}}(\varepsilon)$.¹

We observe that for $p \geq 2$, it holds that $\frac{18p+4}{3p+6} \geq 6 - \frac{16}{3p}$. Hence, the requirement on n to achieve $W_2(\nu_n^{\text{CRLMC}}) = \tilde{\mathcal{O}}(\varepsilon)$ can be simplified to $n = \tilde{\Omega}(\varepsilon^{-6+16/(3p)})$.

¹The notation $\tilde{\mathcal{O}}$ and $\tilde{\Omega}$ suppress the dependence on $\log(1/\varepsilon)$

2.4 Randomized Midpoint Method for Kinetic Langevin Diffusion under Constraints

The randomized midpoint method, introduced in [SL19] provides a discretization of the kinetic Langevin process that reduces sampling bias compared to standard schemes in the unconstrained setting.

Recall that the kinetic Langevin process \mathbf{L}^{KLD} is a solution to the second-order SDE

$$\frac{1}{\gamma} \ddot{\mathbf{L}}_t^{\text{KLD}} + \dot{\mathbf{L}}_t^{\text{KLD}} = -\nabla U^\lambda(\mathbf{L}_t^{\text{KLD}}) + \sqrt{2} \dot{\mathbf{W}}_t,$$

with initial conditions $\mathbf{L}_0^{\text{KLD}} = \boldsymbol{\vartheta}_0$ and $\dot{\mathbf{L}}_0^{\text{KLD}} = \mathbf{v}_0$, where $\gamma > 0$ is the friction parameter and \mathbf{W} is a standard p -dimensional Brownian motion. Dots denote derivatives with respect to time $t \geq 0$. This can be formalized using Itô's calculus and introducing the velocity field \mathbf{V}^{KLD} so that the joint process $(\mathbf{L}^{\text{KLD}}, \mathbf{V}^{\text{KLD}})$ satisfies

$$d\mathbf{L}_t^{\text{KLD}} = \mathbf{V}_t^{\text{KLD}} dt; \quad \frac{1}{\gamma} d\mathbf{V}_t^{\text{KLD}} = -(\mathbf{V}_t^{\text{KLD}} + \nabla U^\lambda(\mathbf{L}_t^{\text{KLD}})) dt + \sqrt{2} d\mathbf{W}_t. \quad (2.5)$$

Similar to the vanilla Langevin diffusion (2.3), this Markov process is ergodic when the potential U^λ is strongly convex [EGZ19], and admits the invariant density

$$p_*(\boldsymbol{\theta}, \mathbf{v}) \propto \exp \left\{ -U^\lambda(\boldsymbol{\theta}) - \frac{1}{2\gamma} \|\mathbf{v}\|^2 \right\}, \quad \text{for all } \boldsymbol{\theta}, \mathbf{v} \in \mathbb{R}^p.$$

whose marginal in $\boldsymbol{\theta}$ recovers the target distribution ν^λ . Notably, the distribution of \mathbf{L}^{KLD} approaches that of the vanilla Langevin process \mathbf{L}^{LD} as γ approaches infinity (see e.g. [Nel67]).

To discretize this continuous-time process for sampling from ν^λ , we apply the midpoint randomization scheme to the kinetic Langevin diffusion. The resulting algorithm, termed CRKLMC, is applied at each iteration $k = 1, 2, \dots$

- **Step 1:** sample a uniform random variable $\iota_k \sim \text{Unif}[0, 1]$ and random vectors $(\boldsymbol{\xi}'_k, \boldsymbol{\xi}''_k, \boldsymbol{\xi}'''_k)$ such that, conditional on $\iota_k = u$, their joint distribution matches

$$(\mathbf{B}_u - e^{-\gamma h u} \mathbf{G}_u, \mathbf{B}_1 - e^{-\gamma h} \mathbf{G}_1, \gamma e^{-\gamma h} \mathbf{G}_1),$$

where \mathbf{B} is a p -dimensional Brownian motion and $\mathbf{G}_t = \int_0^t e^{\gamma h s} d\mathbf{B}_s$.

- **Step 2:** let $\psi(x) = (1 - e^{-x})/x$ and define the $(k+1)$ -th iterate of CRKLMC by

$$\begin{aligned} \boldsymbol{\vartheta}_{k+\iota}^{\text{CRKLMC}} &= \boldsymbol{\vartheta}_k^{\text{CRKLMC}} + \iota_k h \psi(\gamma h \iota_k) \mathbf{v}_k^{\text{CRKLMC}} - \iota_k h (1 - \psi(\gamma h \iota_k)) \nabla U^\lambda(\boldsymbol{\vartheta}_k^{\text{CRKLMC}}) + \sqrt{2h} \boldsymbol{\xi}'_k \\ \boldsymbol{\vartheta}_{k+1}^{\text{CRKLMC}} &= \boldsymbol{\vartheta}_k^{\text{CRKLMC}} + h \psi(\gamma h) \mathbf{v}_k^{\text{CRKLMC}} - \gamma h^2 (1 - \iota_k) \psi(\gamma h (1 - \iota_k)) \nabla U^\lambda(\boldsymbol{\vartheta}_{k+\iota}^{\text{CRKLMC}}) + \sqrt{2h} \boldsymbol{\xi}''_k \\ \mathbf{v}_{k+1}^{\text{CRKLMC}} &= e^{-\gamma h} \mathbf{v}_k^{\text{CRKLMC}} - \gamma h e^{-\gamma h (1 - \iota_k)} \nabla U^\lambda(\boldsymbol{\vartheta}_{k+\iota}^{\text{CRKLMC}}) + \sqrt{2h} \boldsymbol{\xi}'''_k. \end{aligned}$$

The following theorem provides the choice of λ , step size h , and the number of iterations n needed for CRKLMC to ensure that the distribution ν_n^{CRKLMC} of the n -th iterate $\boldsymbol{\vartheta}_n^{\text{CRKLMC}}$ is within error ε of the target ν .

Theorem 4. Under Assumptions 1- 4, let the error level $\varepsilon \in (0, 1)$ be small. Set $\gamma = 5(M + M_0/\lambda^2)$. The initial point $\boldsymbol{\vartheta}_0^{\text{CRKLMC}}$ is set to be the minimizer of the function f and $\mathbf{v}_0^{\text{CRKLMC}} \sim \mathcal{N}_p(0, \gamma \mathbf{I}_p)$.
(a) Set $\lambda = \Theta(h^{6p/(15p+2)})$, and choose $h > 0$ and $n \in \mathbb{N}_+$ so that

$$h = \mathcal{O}\left(\varepsilon^{\frac{15p+2}{3p+6}}\right) \quad \text{and} \quad n = \tilde{\Omega}\left(\varepsilon^{-\frac{15p+2}{3p+6}}\right)$$

then we have $W_2(\nu_n^{\text{CRKLMC}}) = \tilde{\mathcal{O}}(\varepsilon)$.

(b) Set $\lambda = \Theta(h^{3/8})$, and choose $h > 0$ and $n \in \mathbb{N}_+$ so that

$$h = \mathcal{O}\left(\varepsilon^{\frac{8}{3}}\right) \quad \text{and} \quad n = \tilde{\Omega}\left(\varepsilon^{-\frac{8}{3}}\right)$$

then we have $W_1(\nu_n^{\text{CRKLMC}}) = \tilde{\mathcal{O}}(\varepsilon)$.

When $p \geq 2$, it holds that $\frac{15p+2}{3p+6} \geq 5 - \frac{14}{3p}$. This implies the requirement on the number of iterations n for achieving $W_2(\nu_n^{\text{CRKLMC}}) = \tilde{\mathcal{O}}(\varepsilon)$ can be relaxed to $n = \tilde{\Omega}(\varepsilon^{-5+14/(3p)})$.

2.5 Improved Error Bounds for Constrained Langevin and Kinetic Langevin Monte Carlo

The refined analysis of $W_q(\nu, \nu^\lambda)$ from the previous section allows us to derive improved upper bounds on the error of the LMC and KLMC algorithms in the constrained setting considered in this work, termed CLMC, CKLMC. Specifically, CLMC is described in (2.4), while CKLMC corresponds to a discretization of the SDE in (2.5), as studied in [GHZ24], where the drift term $\nabla U^\lambda(\mathbf{L}_t)$ is replaced by $\nabla U^\lambda(\mathbf{L}_{kh})$ over each interval $[kh, (k+1)h]$. The resulting error bounds, stated in the following theorems, demonstrate improved dependence on the target accuracy level ε compared to previously established results.

The following theorem presents the improved Wasserstein convergence rate for the CLMC algorithm.

Theorem 5. *Under Assumptions 1- 4, let the error level $\varepsilon \in (0, 1)$ be small, set the initial distribution ν_0^{CLMC} of $\vartheta_0^{\text{CLMC}}$ as the Dirac measure concentrated at the minimizer of the function f .*

(a) Set $\lambda = \Theta(h^{p/(3p+2)})$, and choose $h > 0$ and $n \in \mathbb{N}_+$ so that

$$h = \mathcal{O}\left(\varepsilon^{\frac{6p+4}{p+2}}\right) \quad \text{and} \quad n = \tilde{\Omega}\left(\varepsilon^{-\frac{6p+4}{p+2}}\right),$$

then we have $W_2(\nu_n^{\text{CLMC}}, \nu) = \tilde{\mathcal{O}}(\varepsilon)$.

(b) Set $\lambda = \Theta(h^{1/4})$, choose $h > 0$ and $n \in \mathbb{N}_+$ so that

$$h = \mathcal{O}(\varepsilon^4) \quad \text{and} \quad n = \tilde{\Omega}(\varepsilon^{-4}),$$

then we have $W_1(\nu_n^{\text{CLMC}}, \nu) = \tilde{\mathcal{O}}(\varepsilon)$.

According to this theorem, the CLMC algorithm requires $\tilde{\mathcal{O}}(\varepsilon^{-4})$ gradient evaluations to achieve a target accuracy ε in W_1 distance. This improves upon the rate $\tilde{\mathcal{O}}(\varepsilon^{-6})$ obtained in [BDMP17]. Moreover, we note that $\frac{6p+4}{p+2} \geq 6 - \frac{4}{p}$ holds when $p \geq 2$. Thus, the requirement on n to achieve $W_2(\nu_n^{\text{CLMC}}, \nu) = \tilde{\mathcal{O}}(\varepsilon)$ can be simplified to $n = \tilde{\Omega}(\varepsilon^{-6+4/p})$. This rate $\tilde{\mathcal{O}}(\varepsilon^{-6+4/p})$, significantly improves upon the result $\tilde{\mathcal{O}}(\varepsilon^{-18})$ from Proposition 2.21 of [GHZ24], obtained under the zero-variance assumption $\sigma = 0$ for the stochastic gradient (i.e., the deterministic gradient setting). The improvement in convergence rates primarily results from our tighter bound on $W_q(\nu, \nu^\lambda)$. We also note that both [BDMP17, GHZ24] focus on Euclidean projection, which is a special case within our framework.

Furthermore, comparing the convergence rate of CLMC with that of CRLMC in Theorem 3, we observe that the midpoint randomization yields a clear acceleration over the Euler discretization.

The following theorem presents improved Wasserstein error bounds for the CKLMC algorithm. Let ν_n^{CKLMC} denote the distribution of $\vartheta_n^{\text{CKLMC}}$.

Theorem 6. Under Assumptions 1- 4, let the error level $\varepsilon \in (0, 1)$ be small. Set $\gamma = 5(M + M_0/\lambda^2)$. Initialize the algorithm with $\vartheta_0^{\text{CKLMC}}$ set to the minimizer of f , and $\mathbf{v}_0^{\text{CKLMC}} \sim \mathcal{N}_p(0, \gamma \mathbf{I}_p)$.

(a) Set $\lambda = \Theta(h^{2p/(7p+2)})$, and choose $h > 0$ and $n \in \mathbb{N}_+$ so that

$$h = \mathcal{O}\left(\varepsilon^{\frac{7p+2}{p+2}}\right) \quad \text{and} \quad n = \tilde{\Omega}\left(\varepsilon^{-\frac{7p+2}{p+2}}\right)$$

then we have $W_2(\nu_n^{\text{CKLMC}}, \nu) = \tilde{\mathcal{O}}(\varepsilon)$.

(b) Set $\lambda = \Theta(h^{1/4})$, and choose $h > 0$ and $n \in \mathbb{N}_+$ so that

$$h = \mathcal{O}(\varepsilon^4) \quad \text{and} \quad n = \tilde{\Omega}(\varepsilon^{-4})$$

then we have $W_1(\nu_n^{\text{CKLMC}}, \nu) = \tilde{\mathcal{O}}(\varepsilon)$.

When $p \geq 2$, we have $\frac{7p+2}{p+2} \geq 7 - \frac{6}{p}$. This allows us to simplify the requirement on the number of iterations n needed to achieve $W_2(\nu_n^{\text{CKLMC}}, \nu) = \tilde{\mathcal{O}}(\varepsilon)$ to $n = \tilde{\Omega}(\varepsilon^{-7+6/p})$. A comparable convergence rate $\tilde{\mathcal{O}}(\varepsilon^{-13})$ in W_2 distance can be derived from Proposition 2.22 in [GHZ24] by setting the stochastic gradient variance $\sigma = 0$, which recovers the deterministic gradient setting considered in our work. This improvement is primarily attributed to the tighter bound on $W_2(\nu, \nu^\lambda)$.

A comparison of the convergence rates of CKLMC and CRKLMC in Theorem 4 reveals that the midpoint randomization scheme provides a clear acceleration over the Euler discretization.

3 Numerical Experiments

In this section, we compare the performance of the CLMC, CKLMC, CRLMC, and CRKLMC algorithms to support our theoretical findings.

Due to the difficulty of computing high-dimensional Wasserstein distances, we focus on a two-dimensional setting in this section to facilitate clearer presentation and easier visualization. Specifically, we consider the 2-dimensional standard normal distribution $\mathcal{N}(0, \mathbf{I}_2)$ and construct the target distribution ν by imposing two different choices for the constraint set \mathcal{K} .

The first setting uses a Euclidean ball centered at the origin, defined as $\mathcal{K} := \mathcal{B}_2(0, r)$ with $r = 0.5$. In this case, we employ Euclidean projection, which coincides with the Gauge projection due to the symmetry of the constraint set. The second setting significantly differs from the first. Here, \mathcal{K} is defined as a 3-simplex shifted away from the origin: $\mathcal{K} := \{(x_1, x_2) \in \mathbb{R}^2 : x_1, x_2 \geq -0.3, x_1 + x_2 \leq 0.6\}$. Here, we apply the Gauge projection to enforce the constraint.

Each algorithm is run for n iterations. At the final iteration, N samples are drawn from the approximate distribution to compare against the true target ν . We use a step size of $h = 0.001$ (scaled by a factor of 0.1 when the samples lie within \mathcal{K}), and set the tuning parameters as follows

$$\lambda^{\text{CLMC}} = h^{1/4}, \quad \lambda^{\text{CRLMC}} = h^{1/4}, \quad \lambda^{\text{CKLMC}} = h^{3/10}, \quad \lambda^{\text{CRKLMC}} = h^{3/8}.$$

Figures 1 and 2 display scatter plots of the generated samples for both constraint sets with $n = 1000$ and $N = 500$. The red dashed lines in the plots indicate the boundaries of the constraint sets. The visualizations offer valuable intuition and a qualitative sense of convergence. They indicate that CRKLMC achieves the best performance, with samples more tightly concentrated within the constraint set. CRLMC outperforms CLMC, and CRKLMC improves upon CKLMC, highlighting the advantage of midpoint randomization over Euler discretization. These observations align well with our theoretical findings. Additional results with different combinations of n and N , along with implementation details, are provided in Appendix E. The supplementary plots exhibit trends consistent with the observations discussed in this section

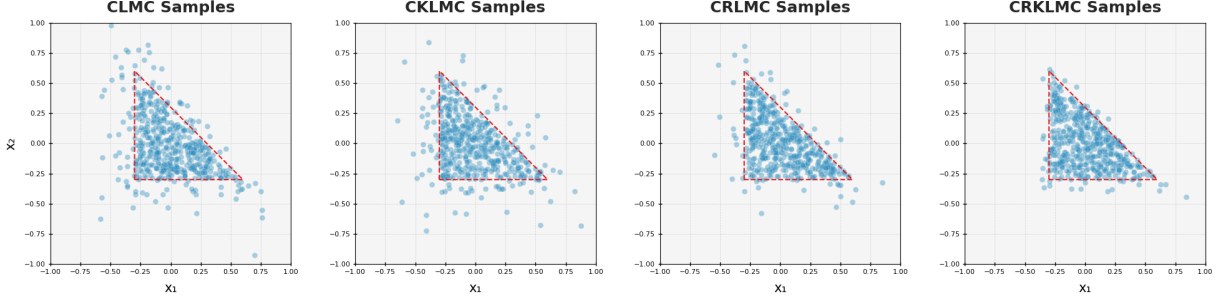


Figure 1: Scatter plots of samples generated by {CL,CKL,CRL,CRKL}MC algorithms.

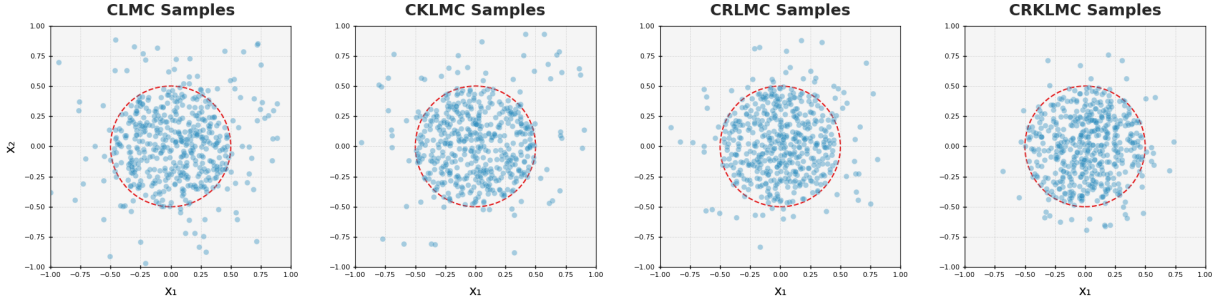


Figure 2: Scatter plots of samples generated by {CL,CKL,CRL,CRKL}MC algorithms.

4 Discussion

In this work, we adopt the Wasserstein distance as the primary metric for measuring sampling error, given its natural connection to optimal transport theory. However, recent advancements in gradient-based sampling have investigated other metrics, including total variation distance, KL divergence, and χ^2 divergence. Extending guarantees for constrained sampling to these alternative metrics presents an interesting direction for future research.

In addition, while our focus has been on midpoint randomization for both vanilla and kinetic Langevin Monte Carlo in constrained settings, investigating parallelized variants of these algorithms under constraints is another promising avenue.

Finally, in many practical scenarios, computing exact gradients may be computationally expensive or infeasible. Exploring constrained sampling in settings where only noisy and stochastic gradient evaluations are available would also be an interesting direction.

5 Acknowledgments

We are grateful to Arnak Dalalyan for inspiring discussions and constructive comments during the early stages of this manuscript. Part of this work was done when LY was a postdoctoral researcher at CREST/ENSAE Paris, supported by the center Hi! PARIS.

References

- [AC21] Kwangjun Ahn and Sinho Chewi, *Efficient constrained sampling via the mirror-langevin algorithm*, Advances in Neural Information Processing Systems **34** (2021), 28405–28418.

- [ADFDJ03] Christophe Andrieu, Nando De Freitas, Arnaud Doucet, and Michael I Jordan, *An introduction to mcmc for machine learning*, Machine learning **50** (2003), 5–43.
- [BDMP17] Nicolas Brosse, Alain Durmus, Éric Moulines, and Marcelo Pereyra, *Sampling from a log-concave distribution with compact support with proximal langevin monte carlo*, Conference on learning theory, PMLR, 2017, pp. 319–342.
- [BEL15] Sébastien Bubeck, Ronen Eldan, and Joseph Lehec, *Finite-time analysis of projected langevin monte carlo*, Advances in Neural Information Processing Systems **28** (2015).
- [BEL18] Sébastien Bubeck, Ronen Eldan, and Joseph Lehec, *Sampling from a log-concave distribution with projected langevin monte carlo*, Discrete & Computational Geometry **59** (2018), no. 4, 757–783.
- [Bha78] R. N. Bhattacharya, *Criteria for recurrence and existence of invariant measures for multidimensional diffusions*, Ann. Probab. **6** (1978), no. 4, 541–553.
- [BSU12] Marcus Brubaker, Mathieu Salzmann, and Raquel Urtasun, *A family of mcmc methods on implicitly defined manifolds*, Artificial intelligence and statistics, PMLR, 2012, pp. 161–172.
- [CKJK24] Luiz Chamon, Mohammad Reza Karimi Jaghargh, and Anna Korba, *Constrained sampling with primal-dual langevin monte carlo*, Advances in Neural Information Processing Systems **37** (2024), 29285–29323.
- [CLGL⁺20] Sinho Chewi, Thibaut Le Gouic, Chen Lu, Tyler Maunu, Philippe Rigollet, and Austin Stromme, *Exponential ergodicity of mirror-langevin diffusions*, Advances in Neural Information Processing Systems **33** (2020), 19573–19585.
- [Dal17] Arnak S. Dalalyan, *Theoretical guarantees for approximate sampling from a smooth and log-concave density*, J. R. Stat. Soc. B **79** (2017), 651 – 676.
- [DFK91] Martin Dyer, Alan Frieze, and Ravi Kannan, *A random polynomial-time algorithm for approximating the volume of convex bodies*, Journal of the ACM (JACM) **38** (1991), no. 1, 1–17.
- [DM17] Alain Durmus and Eric Moulines, *Nonasymptotic convergence analysis for the unadjusted Langevin algorithm*, Ann. Appl. Probab. **27** (2017), no. 3, 1551–1587.
- [DM19] Alain Durmus and Éric Moulines, *High-dimensional Bayesian inference via the unadjusted Langevin algorithm*, Bernoulli **25** (2019), no. 4A, 2854 – 2882.
- [DMM19] Alain Durmus, Szymon Majewski, and Błażej Miasojedow, *Analysis of langevin monte carlo via convex optimization*, The Journal of Machine Learning Research **20** (2019), no. 1, 2666–2711.
- [DMP18] Alain Durmus, Eric Moulines, and Marcelo Pereyra, *Efficient bayesian computation by proximal markov chain monte carlo: when langevin meets moreau*, SIAM Journal on Imaging Sciences **11** (2018), no. 1, 473–506.
- [DRD20] Arnak S Dalalyan and Lionel Riou-Durand, *On sampling from a log-concave density using kinetic Langevin diffusions*, Bernoulli **26** (2020), no. 3, 1956–1988.

- [EGZ19] Andreas Eberle, Arnaud Guillin, and Raphael Zimmer, *Couplings and quantitative contraction rates for Langevin dynamics*, Ann. Probab. **47** (2019), no. 4, 1982–2010.
- [EH21] Murat A Erdogdu and Rasa Hosseinzadeh, *On the convergence of langevin monte carlo: The interplay between tail growth and smoothness*, COLT 2021, 2021.
- [EHZ22] Murat A Erdogdu, Rasa Hosseinzadeh, and Shunshi Zhang, *Convergence of langevin monte carlo in chi-squared and rényi divergence*, AISTATS 2022, 2022.
- [Ein05] Albert Einstein, *Über die von der molekularkinetischen theorie der wärme geforderte bewegung von in ruhenden flüssigkeiten suspendierten teilchen*, Annalen der physik **4** (1905).
- [EMS18] Murat A Erdogdu, Lester Mackey, and Ohad Shamir, *Global non-convex optimization with discretized diffusions*, Advances in Neural Information Processing Systems (S. Bengio, H. Wallach, H. Larochelle, K. Grauman, N. Cesa-Bianchi, and R. Garnett, eds.), vol. 31, Curran Associates, Inc., 2018.
- [GCC24] Shivam Gupta, Linda Cai, and Sitan Chen, *Faster diffusion-based sampling with randomized midpoints: Sequential and parallel*, arXiv preprint arXiv:2406.00924 (2024).
- [GCSR95] Andrew Gelman, John B Carlin, Hal S Stern, and Donald B Rubin, *Bayesian data analysis*, Chapman and Hall/CRC, 1995.
- [Gho19] Hamid Ghorbani, *Mahalanobis distance and its application for detecting multivariate outliers*, Facta Universitatis, Series: Mathematics and Informatics (2019), 583–595.
- [GHZ24] Mert Gurbuzbalaban, Yuanhan Hu, and Lingjiong Zhu, *Penalized overdamped and underdamped langevin monte carlo algorithms for constrained sampling*, Journal of Machine Learning Research **25** (2024), no. 263, 1–67.
- [GPAM⁺14] Ian Goodfellow, Jean Pouget-Abadie, Mehdi Mirza, Bing Xu, David Warde-Farley, Sherjil Ozair, Aaron Courville, and Yoshua Bengio, *Generative adversarial nets*, Advances in neural information processing systems **27** (2014).
- [GSL92] Alan E Gelfand, Adrian FM Smith, and Tai-Ming Lee, *Bayesian analysis of constrained parameter and truncated data problems using gibbs sampling*, Journal of the American Statistical Association **87** (1992), no. 418, 523–532.
- [HBE20] Ye He, Krishnakumar Balasubramanian, and Murat A Erdogdu, *On the ergodicity, bias and asymptotic normality of randomized midpoint sampling method*, Advances in Neural Information Processing Systems **33** (2020), 7366–7376.
- [HKRC18] Ya-Ping Hsieh, Ali Kavis, Paul Rolland, and Volkan Cevher, *Mirrored langevin dynamics*, Advances in Neural Information Processing Systems **31** (2018).
- [KLS97] Ravi Kannan, László Lovász, and Miklós Simonovits, *Random walks and an $o^*(n^5)$ volume algorithm for convex bodies*, Random Structures & Algorithms **11** (1997), no. 1, 1–50.
- [KLSV22] Yunbum Kook, Yin-Tat Lee, Ruqi Shen, and Santosh Vempala, *Sampling with riemannian hamiltonian monte carlo in a constrained space*, Advances in Neural Information Processing Systems **35** (2022), 31684–31696.

- [KVZ24] Yunbum Kook, Santosh S Vempala, and Matthew S Zhang, *In-and-out: Algorithmic diffusion for sampling convex bodies*, arXiv preprint arXiv:2405.01425 (2024).
- [KW13] Diederik P Kingma and Max Welling, *Auto-encoding variational bayes*, arXiv preprint arXiv:1312.6114 (2013).
- [Lam21] Andrew Lamperski, *Projected stochastic gradient langevin algorithms for constrained sampling and non-convex learning*, Conference on Learning Theory, PMLR, 2021, pp. 2891–2937.
- [LBGH22] Zhou Lu, Nataly Brukhim, Paula Gradu, and Elad Hazan, *Projection-free adaptive regret with membership oracles*, arXiv preprint arXiv:2211.12638 (2022).
- [Leh23] Joseph Lehec, *The langevin monte carlo algorithm in the non-smooth log-concave case*, The Annals of Applied Probability **33** (2023), no. 6A, 4858–4874.
- [LJ24] Gen Li and Yuchen Jiao, *Improved convergence rate for diffusion probabilistic models*, arXiv preprint arXiv:2410.13738 (2024).
- [LLK⁺22] Lingxiao Li, Qiang Liu, Anna Korba, Mikhail Yurochkin, and Justin Solomon, *Sampling with mollified interaction energy descent*, arXiv preprint arXiv:2210.13400 (2022).
- [Lov99] László Lovász, *Hit-and-run mixes fast*, Mathematical programming **86** (1999), 443–461.
- [LS93] László Lovász and Miklós Simonovits, *Random walks in a convex body and an improved volume algorithm*, Random structures & algorithms **4** (1993), no. 4, 359–412.
- [LV07] László Lovász and Santosh Vempala, *The geometry of logconcave functions and sampling algorithms*, Random Structures & Algorithms **30** (2007), no. 3, 307–358.
- [MFWB22] Wenlong Mou, Nicolas Flammarion, Martin J Wainwright, and Peter L Bartlett, *Improved bounds for discretization of Langevin diffusions: Near-optimal rates without convexity*, Bernoulli **28** (2022), no. 3, 1577–1601.
- [Mha22] Zakaria Mhammedi, *Efficient projection-free online convex optimization with membership oracle*, Conference on Learning Theory, PMLR, 2022, pp. 5314–5390.
- [MHFH⁺23] Alireza Mousavi-Hosseini, Tyler Farghly, Ye He, Krishnakumar Balasubramanian, and Murat A Erdogdu, *Towards a Complete Analysis of Langevin Monte Carlo: Beyond Poincaré Inequality*, arXiv preprint arXiv:2303.03589 (2023).
- [Nel67] Edward Nelson, *Dynamical theories of brownian motion*, Department of Mathematics, Princeton University, 1967.
- [OHHDT22] Joaquim Ortiz-Haro, Jung-Su Ha, Danny Driess, and Marc Toussaint, *Structured deep generative models for sampling on constraint manifolds in sequential manipulation*, Conference on Robot Learning, PMLR, 2022, pp. 213–223.
- [Per16] Marcelo Pereyra, *Proximal markov chain monte carlo algorithms*, Statistics and Computing **26** (2016), 745–760.
- [RRT17] Maxim Raginsky, Alexander Rakhlin, and Matus Telgarsky, *Non-convex learning via stochastic gradient langevin dynamics: a nonasymptotic analysis*, COLT 2017, 2017.

- [RT96] G. O. Roberts and R. L. Tweedie, *Exponential convergence of Langevin distributions and their discrete approximations*, Bernoulli **2** (1996), no. 4, 341–363. MR 1440273 (98j:62014)
- [RW09] R Tyrrell Rockafellar and Roger J-B Wets, *Variational analysis*, vol. 317, Springer Science & Business Media, 2009.
- [SL19] Ruoqi Shen and Yin Tat Lee, *The randomized midpoint method for log-concave sampling*, Advances in Neural Information Processing Systems **32** (2019).
- [Smi84] Robert L Smith, *Efficient monte carlo procedures for generating points uniformly distributed over bounded regions*, Operations Research **32** (1984), no. 6, 1296–1308.
- [SR20] Adil Salim and Peter Richtárik, *Primal dual interpretation of the proximal stochastic gradient langevin algorithm*, Advances in Neural Information Processing Systems **33** (2020), 3786–3796.
- [Stu10] Andrew M Stuart, *Inverse problems: a bayesian perspective*, Acta numerica **19** (2010), 451–559.
- [Vil09] Cédric Villani, *Optimal transport: old and new*, vol. 338, Springer, 2009.
- [VS06] Marian Von Smoluchowski, *Zur kinetischen theorie der brownschen molekularbewegung und der suspensionen*, Annalen der physik **326** (1906), no. 14, 756–780.
- [XJRN02] Eric Xing, Michael Jordan, Stuart J Russell, and Andrew Ng, *Distance metric learning with application to clustering with side-information*, Advances in neural information processing systems **15** (2002).
- [XNZ08] Shiming Xiang, Feiping Nie, and Changshui Zhang, *Learning a mahalanobis distance metric for data clustering and classification*, Pattern recognition **41** (2008), no. 12, 3600–3612.
- [YD24] Lu Yu and Arnak Dalalyan, *Parallelized midpoint randomization for langevin monte carlo*, arXiv preprint arXiv:2402.14434 (2024).
- [YKD23] Lu Yu, Avetik Karagulyan, and Arnak Dalalyan, *Langevin monte carlo for strongly log-concave distributions: Randomized midpoint revisited*, arXiv preprint arXiv:2306.08494 (2023).
- [YY25] Yifeng Yu and Lu Yu, *Advancing wasserstein convergence analysis of score-based models: Insights from discretization and second-order acceleration*, arXiv preprint arXiv:2502.04849 (2025).
- [ZPFP20] Kelvin Shuangjian Zhang, Gabriel Peyré, Jalal Fadili, and Marcelo Pereyra, *Wasserstein control of mirror langevin monte carlo*, Conference on Learning Theory, PMLR, 2020, pp. 3814–3841.

A Relation to Works [BDMP17] and [GHZ24]

These two works follow a similar two-stage procedure to ours: they introduce a regularity term to construct a smooth surrogate density, which is then sampled using Langevin Monte Carlo (LMC) and/or kinetic Langevin Monte Carlo (KLMC). Below, we provide a detailed discussion of their results and highlight the key differences from our approach.

A.1 Comparison with [BDMP17]

[BDMP17] considers the same setting as the current study, proposing the use of the Moreau envelope (Example 2.1 with $Q = I$) to derive a smooth surrogate density, followed by applying LMC to sample from this density. Their approach supports our general framework, which integrates Euclidean projection with LMC, and provides convergence bounds in both the W_1 metric and total variation distance. In contrast, our analysis is conducted in the Wasserstein distance and accommodates a broader class of projection operators beyond the Euclidean case, as well as a wider range of sampling algorithms beyond vanilla Langevin Monte Carlo.

A.2 Comparison with the concurrent work [GHZ24]

Upon completing the first version of this work, we came across an updated version of [GHZ24], where the authors study the behavior of LMC and KLMC for constrained sampling. Similar to our approach, they reformulate the constrained sampling problem as an unconstrained one by introducing a penalty function. Similar to [BDMP17], they make use of the Euclidean projection.

However, their focus differs from ours in two key ways:

1. They analyze convergence in total variation distance and allow the objective function f to be smooth and possibly non-convex.
2. They consider settings with access to stochastic gradients and derive W_2 error bounds for constrained LMC and KLMC. Specifically, when f is strongly convex and smooth, the W_2 convergence rates are of order $\mathcal{O}(\varepsilon^{-18})$ for constrained LMC and $\mathcal{O}(\varepsilon^{-39})$ for constrained KLMC. They also extend their analysis of W_2 error bounds to the non-convex case, under smoothness assumptions on the potential f .

To obtain a comparable counterpart in their work, we consider the second setting where f is strongly convex and smooth, and additionally assume that the stochastic gradient has zero variance, corresponding to the deterministic gradient setting considered in our analysis. The corresponding convergence rates are detailed in Section 2.5. Our results significantly improve upon the convergence rates established in [GHZ24], with the improvement primarily due to a tighter bound on the Wasserstein distance between the surrogate density and the target distribution.

A.3 Summary

In summary, our work extends the two-stage approach by introducing a general framework that accommodates a broader class of projection methods and sampling algorithms beyond LMC and KLMC. This enhances the applicability of methods such as RLMC and RKLMC in constrained settings. Moreover, our sharper analysis in the first stage, which tightly bounds the gap between the surrogate and target densities, leads to improved convergence rates compared to existing results for constrained LMC and KLMC.

B Proofs of Section 2.1

In this part, we provide the proof of Proposition 1 and Proposition 2.

Additional Notation. Throughout the remainder, for any set $\mathcal{K} \subset \mathbb{R}^p$, we denote its complement by \mathcal{K}^c , and its volume by $\text{Vol}(\mathcal{K})$. \mathbb{S}_{p-1} denotes the unit sphere in \mathbb{R}^p , ω_{p-1} denotes the $(p-1)$ -dimensional surface area of \mathbb{S}_{p-1} , and V_p the volume of the p -dimensional unit ball.

B.1 Proof of Proposition 1

High-Level Intuition. We introduce a new proof strategy based on a carefully constructed transport map that aligns the radial distribution of the surrogate distribution ν^λ with that of the target distribution ν . This map, denoted T , is designed in polar coordinates so that $T_\# \nu^\lambda$ closely approximates ν . By leveraging the radial alignment, we achieve a more precise and structured quantification of the Wasserstein distance between ν^λ and ν .

More specifically, we bound the Wasserstein distance $W_q(\nu, \nu^\lambda)$ via the following decomposition

$$W_q(\nu, \nu^\lambda) \leq W_q(\nu, T_\# \nu^\lambda) + W_q(T_\# \nu^\lambda, \nu^\lambda),$$

and analyze each term separately. The first term accounts for the discrepancy between ν and $T_\# \nu$, which only arises in a small neighborhood near the origin. Outside this region, the transport map T exactly aligns the two distributions. The second term captures the cost of transporting ν^λ under the map T , and is decomposed into three radial regions: an interior region near the origin, a near-boundary region where the discrepancy in radial coordinates is small but non-negligible, and an exterior region outside the set \mathcal{K} . This structured analysis leads to sharp, non-asymptotic bounds on the Wasserstein distance.

Proof. [Proof of Proposition 1] In polar coordinates, any vector $x \in \mathbb{R}^p$ can be uniquely expressed as $x = \rho\theta$, where $\rho \geq 0$ is the radial coordinate and $\theta \in \mathbb{S}_{p-1}$ denotes the directional unit vector on the $(p-1)$ -dimensional sphere. For each direction θ , the radial function is defined as

$$R(\theta) := \sup\{r \geq 0 : r\theta \in \mathcal{K}\}.$$

which characterizes the extent of the set \mathcal{K} along direction θ . This parameterization allows us to define the radial cumulative distribution function accordingly.

$$\begin{aligned} F(\rho, \theta) &:= \frac{\int_0^\rho t^{p-1} e^{-f(t\theta)} dt}{\int_{\mathcal{K}} e^{-f(x)} dx}, \quad \rho \in [0, R(\theta)], \\ F_\lambda(\rho, \theta) &:= \frac{\int_0^\rho t^{p-1} e^{-f(t\theta) - \frac{1}{2\lambda^2} d_{\mathcal{K}}(t\theta)} dt}{\int_{\mathcal{K}} e^{-f(x)} dx + \int_{\mathcal{K}^c} e^{-f(x) - \frac{1}{2\lambda^2} d_{\mathcal{K}}(x)} dx}, \quad \rho \in [0, \infty). \end{aligned}$$

Define

$$Z := \int_{\mathcal{K}} e^{-f(x)} dx \quad \text{and} \quad Z_\lambda := Z + \int_{\mathcal{K}^c} e^{-U^\lambda(x)} dx.$$

To bound the difference $Z_\lambda - Z$, we need the following lemma.

Lemma 7. *Under Assumptions 1-3, for any $k \geq 0$, if $\lambda < c_1^{1/2} r / (p+k)$, it holds that*

$$\int_{\mathcal{K}^c} \|x\|_2^k e^{-U^\lambda(x)} dx \leq \frac{3\sqrt{\pi}(p+k)e^{-l}}{rc_1^{1/2}} \lambda \times \int_{\mathcal{K}} \|x\|_2^k dx.$$

By Lemma 7, we have

$$Z_\lambda - Z = \int_{\mathcal{K}^c} e^{-U^\lambda(x)} dx \leq \frac{3\sqrt{\pi}pe^{-l}\text{Vol}(\mathcal{K})}{rc_1^{1/2}}\lambda. \quad (\text{B.1})$$

Define $\epsilon(\theta) := F_\lambda(\infty, \theta) - F(R(\theta), \theta)$. The following lemma provides a bound for this term.

Lemma 8. *Assume the assumptions stated in Lemma 7 are satisfied. There exists a universal constant $C_\epsilon(p) > 0$ such that for all $\theta \in \mathbb{S}_{p-1}$, it holds that $|\epsilon(\theta)| \leq C_\epsilon(p)\lambda$, where $C_\epsilon(p) = (a_1 p)^{(p+1)/2}$ and a_1 is constant independent of p and λ .*

By Implicit Function Theorem, there exists two differential function g and $g_\lambda : [0, \infty) \times \mathbb{S}_{p-1} \rightarrow [0, \infty)$, satisfying

$$F(g(c, \theta), \theta) = c, \quad \text{and} \quad F_\lambda(g_\lambda(c, \theta), \theta) = c$$

respectively.

Lemma 9. *Denote the upper bound of f on \mathcal{K} by u , that is $l \leq f(x) \leq u, \forall x \in \mathcal{K}$. The following three properties hold for the functions F, F_λ , and their inverse functions g, g_λ .*

1. For any fixed $\theta \in \mathbb{S}_{p-1}$, $g(x, \theta)$ and $g_\lambda(x, \theta)$ are both increasing functions with respect to x .
2. For $\rho \leq R(\theta)$, we have

$$\rho^p e^{-u}/(pZ) \leq F(\rho, \theta) \leq \rho^p e^{-l}/(pZ)$$

and

$$\rho^p e^{-u}/(pZ_\lambda) \leq F_\lambda(\rho, \theta) \leq \rho^p e^{-l}/(pZ_\lambda).$$

Thus, it holds that

$$x^{1/p}(pZe^l)^{1/p} \leq g(x, \theta) \leq x^{1/p}(pZe^u)^{1/p} \quad \text{and} \quad x^{1/p}(pZ_\lambda e^l)^{1/p} \leq g_\lambda(x, \theta) \leq x^{1/p}(pZ_\lambda e^u)^{1/p}.$$

3. For $\rho \leq R(\theta)$, we have $F(\rho, \theta) = F_\lambda(\rho, \theta) \cdot Z_\lambda/Z$, therefore, it holds that

$$g(x, \theta) = g_\lambda(x \cdot Z/Z_\lambda, \theta), \quad \forall x \leq F(R(\theta), \theta).$$

Define a deterministic transport map T of the form

$$T(\rho\theta) = g(\max\{F_\lambda(\rho, \theta) - \epsilon(\theta), 0\}, \theta).$$

We decompose the Wasserstein distance between ν and ν^λ into two components

$$\mathbb{W}_q(\nu, \nu^\lambda) \leq \mathbb{W}_q(\nu, T_\#(\nu^\lambda)) + \mathbb{W}_q(T_\#(\nu^\lambda), \nu^\lambda). \quad (\text{B.2})$$

In the following, we derive upper bounds for the two terms on the right-hand side.

Define two sets centered around the origin as

$$\mathcal{K}_0 := \{\rho\theta : \rho \leq g(\max\{-\epsilon(\theta), 0\}, \theta)\}$$

and

$$\mathcal{K}_{0,\lambda} := \{\rho\theta : \rho \leq g_\lambda(\max\{0, \epsilon(\theta)\}, \theta)\}.$$

We note that

$$T_{\#}(\nu^{\lambda}|_{\mathcal{K}_{0,\lambda}^c}) = \nu|_{\mathcal{K}_0^c}.$$

The first term on the right-hand side of display (B.2) can then be bounded by

$$W_q^q(\nu, T_{\#}(\nu^{\lambda})) \leq \int_{\mathcal{K}_0} \text{diam}(\mathcal{K}_0)^q \nu(dx) = \text{diam}(\mathcal{K}_0)^q \nu(\mathcal{K}_0) \quad (\text{B.3})$$

We note that

$$\text{diam}(\mathcal{K}_0) \leq 2 \sup_{\theta \in \mathbb{S}_{p-1}} g(\max\{-\epsilon(\theta), 0\}, \theta) \leq 2 \sup_{\theta \in \mathbb{S}_{p-1}} g(|\epsilon(\theta)|, \theta).$$

By Lemma 8 and Lemma 9, we have

$$g(|\epsilon(\theta)|, \theta) \leq |\epsilon(\theta)|^{1/p} (pZe^u)^{1/p} \leq \lambda^{1/p} (pC_{\epsilon}(p)Ze^u)^{1/p}.$$

This implies

$$\text{diam}(\mathcal{K}_0) \leq 2\lambda^{1/p} (pC_{\epsilon}(p)Ze^u)^{1/p}.$$

Moreover, it holds that

$$\nu(\mathcal{K}_0) \leq e^{-l} \text{Vol}(\mathcal{K}_0)/Z \leq e^{-l} V_p \text{diam}(\mathcal{K}_0)^p / Z \leq e^{\omega(f, \mathcal{K})} \text{diam}(\mathcal{K}_0)^p / r^p,$$

where $\omega(f, \mathcal{K}) := \sup_{x \in \mathcal{K}} f(x) - \inf_{x \in \mathcal{K}} f(x)$ denotes the oscillation of f over \mathcal{K} . Plugging these back to the previous display (B.3) yields

$$\begin{aligned} W_q^q(\nu, T_{\#}(\nu^{\lambda})) &\leq e^{\omega(f, \mathcal{K})} / r^p \cdot \text{diam}(\mathcal{K}_0)^{p+q} \\ &\leq \lambda^{(p+q)/p} e^{\omega(f, \mathcal{K})} / r^p \cdot 2^{p+q} (pC_{\epsilon}(p)Ze^u)^{(p+q)/p}. \end{aligned}$$

Since $Z \leq e^{-l} R^p V_p \leq e^{-l+1/6} R^p (2\pi e)^{p/2} / (\sqrt{\pi} p^{(p+1)/2})$, we finally have

$$\begin{aligned} W_q^q(\nu, T_{\#}(\nu^{\lambda})) &\leq e^{\omega(f, \mathcal{K})} \lambda^{(p+q)/p} \frac{2^{p+q} (a_1^{(p+1)/2} p e^{\omega(f, \mathcal{K})+1/6} R^p (2\pi e)^{p/2})^{(p+q)/p}}{r^p (\sqrt{\pi})^{(p+q)/p}} \\ &\leq a_2^{p+q} p^{(p+q)/p} \lambda^{(p+q)/p}, \end{aligned}$$

where $a_2 = 4\pi e^{2\omega(f, \mathcal{K})+2/3} \max(1, a_1 R) / \min(1, r)$.

We now aim to establish the upper bound for $W_q(T_{\#}(\nu^{\lambda}), \nu^{\lambda})$. Note that

$$\begin{aligned} W_q^q(T_{\#}(\nu^{\lambda}), \nu^{\lambda}) &\leq \int_{\mathbb{S}_{p-1}} \int_0^\infty \|t\theta - T(t\theta)\|_2^q \frac{t^{p-1} e^{-f(t\theta) - \frac{1}{2\lambda^2} d_{\mathcal{K}}(t\theta)}}{\int_{\mathcal{K}} e^{-f(x)} dx + \int_{\mathcal{K}^c} e^{-f(x) - \frac{1}{2\lambda^2} d_{\mathcal{K}}(x)} dx} dt d\theta \\ &= \int_{\mathbb{S}_{p-1}} \underbrace{\int_0^\infty |t - g(\max\{F_{\lambda}(t, \theta) - \epsilon(\theta), 0\}, \theta)|^q \frac{\partial F_{\lambda}(t, \theta)}{\partial t} dt}_{\phi(\theta)} d\theta. \end{aligned}$$

For any fixed $\theta \in \mathbb{S}_{p-1}$, it holds that

$$\begin{aligned}\phi(\theta) &= \underbrace{\int_0^{g_\lambda(\max\{0, \epsilon(\theta)\}, \theta)} |t - g(0, \theta)|^q \frac{\partial F_\lambda(t, \theta)}{\partial t} dt}_{\phi_1(\theta)} \\ &\quad + \underbrace{\int_{g_\lambda(\max\{0, \epsilon(\theta)\}, \theta)}^{R(\theta)} |t - g(F_\lambda(t, \theta) - \epsilon(\theta), \theta)|^q \frac{\partial F_\lambda(t, \theta)}{\partial t} dt}_{\phi_2(\theta)} \\ &\quad + \underbrace{\int_{R(\theta)}^\infty |t - g(F_\lambda(t, \theta) - \epsilon(\theta), \theta)|^q \frac{\partial F_\lambda(t, \theta)}{\partial t} dt}_{\phi_3(\theta)}.\end{aligned}$$

In the following, we derive upper bounds for the three terms ϕ_1, ϕ_2 and ϕ_3 .

Step 1. Since $g(0, \theta) = 0$, we have that

$$\begin{aligned}\int_{\mathbb{S}_{p-1}} \phi_1(\theta) d\theta &= \int_{\mathbb{S}_{p-1}} \int_0^{g_\lambda(\max\{0, \epsilon(\theta)\}, \theta)} t^q \frac{t^{p-1} e^{-f(t\theta) - \frac{1}{2\lambda^2} d_{\mathcal{K}}(t\theta)}}{\int_{\mathcal{K}} e^{-f(x)} dx + \int_{\mathcal{K}^c} e^{-f(x) - \frac{1}{2\lambda^2} d_{\mathcal{K}}(x)} dx} dt d\theta \\ &= \int_{\mathcal{K}_{0,\lambda}} \|x\|_2^q \nu^\lambda(dx) \\ &\leq \text{diam}(\mathcal{K}_{0,\lambda})^q \nu^\lambda(\mathcal{K}_{0,\lambda}) \\ &\leq \text{diam}(\mathcal{K}_{0,\lambda})^q e^{-l} \text{Vol}(\mathcal{K}_{0,\lambda}) / Z_\lambda \\ &\leq \text{diam}(\mathcal{K}_{0,\lambda})^{p+q} e^{\omega(f, \mathcal{K})} / r^p.\end{aligned}$$

Note that

$$\text{diam}(\mathcal{K}_{0,\lambda}) \leq 2 \sup_{\theta \in \mathbb{S}_{p-1}} g_\lambda(|\epsilon(\theta)|, \theta) \leq 2\lambda^{1/p} (pC_\epsilon(p)Z_\lambda e^u)^{1/p}.$$

In addition, when $\lambda = o(r/p)$, it holds that $Z_\lambda < 2Z$. Therefore, we obtain

$$\begin{aligned}\int_{\mathbb{S}_{p-1}} \phi_1(\theta) d\theta &\leq 2^{p+q} (2pC_\epsilon(p)Z_\lambda e^u)^{(p+q)/p} e^{\omega(f, \mathcal{K})} / r^p \times \lambda^{(p+q)/p} \\ &\leq e^{\omega(f, \mathcal{K})} \lambda^{(p+q)/p} \frac{(2^{p+1} p a_1^{(p+1)/2} e^{\omega(f, \mathcal{K})+1/6} R^p (2\pi e)^{p/2})^{(p+q)/p}}{r^p (\sqrt{\pi})^{(p+q)/p}} \\ &\leq a_2^{p+q} p^{(p+q)/p} \lambda^{(p+q)/p}.\end{aligned}$$

Step 2. We now establish the upper bound for $\phi_2(t)$. Let $y = F_\lambda(t, \theta)$. For ease of the notation, we denote the function $h(\cdot, \theta)$ with fixed θ by $h(\cdot|\theta)$. Note that $g(\cdot|\theta) = F^{-1}(\cdot|\theta)$ and $g_\lambda(\cdot|\theta) = F_\lambda^{-1}(\cdot|\theta)$. Using the change of variable, we have

$$\begin{aligned}\phi_2(\theta) &= \int_{\max\{0, \epsilon(\theta)\}}^{F_\lambda(R(\theta)|\theta)} |F_\lambda^{-1}(y|\theta) - F^{-1}(y - \epsilon(\theta)|\theta)|^q dy \\ &= \int_{\max\{0, \epsilon(\theta)\}}^{F_\lambda(R(\theta)|\theta)} |F^{-1}(y \cdot Z_\lambda/Z|\theta) - F^{-1}(y - \epsilon(\theta)|\theta)|^q dy.\end{aligned}$$

The last equality follows from Lemma 9. Then, we decompose the integral into two parts

$$\begin{aligned}\phi_2(\theta) &= \int_{\max\{0, \epsilon(\theta)\}}^{C_\epsilon(p)\lambda} |F^{-1}(y \cdot Z_\lambda/Z|\theta) - F^{-1}(y - \epsilon(\theta)|\theta)|^q dy \\ &\quad + \int_{C_\epsilon(p)\lambda}^{F_\lambda(R(\theta)|\theta)} |F^{-1}(y \cdot Z_\lambda/Z|\theta) - F^{-1}(y - \epsilon(\theta)|\theta)|^q dy.\end{aligned}$$

By Lemma 9 and an application of the mean value theorem to F^{-1} , we obtain

$$\begin{aligned}\phi_2(\theta) &\leq \underbrace{\int_{\max\{0, \epsilon(\theta)\}}^{C_\epsilon(p)\lambda} |(y \cdot Z_\lambda/Z)^{1/p} (pZe^u)^{1/p} + (y - \epsilon(\theta))^{1/p} (pZe^u)^{1/p}|^q dy}_{I_1(\theta)} \\ &\quad + \underbrace{\int_{C_\epsilon(p)\lambda}^{F_\lambda(R(\theta)|\theta)} \left| y \cdot \frac{Z_\lambda - Z}{Z} + \epsilon(\theta) \right|^q \left| \frac{dF^{-1}(z|\theta)}{dz} \right|_{z=\xi}^q dy}_{I_2(\theta)}.\end{aligned}$$

We have

$$\begin{aligned}I_1(\theta) &\leq C_\epsilon(p)\lambda \times |2(2C_\epsilon(p)\lambda)^{1/p} (pZe^u)^{1/p}|^q \\ &\leq \lambda^{(p+q)/p} \times 2^q C_\epsilon(p) (2pC_\epsilon(p)Ze^u)^{q/p} \\ &\leq \lambda^{(p+q)/p} \times 2^q (a_1 p)^{(p+1)/2} (2a_1^{(p+1)/2} p e^{\omega(f, \mathcal{K})+1/6} R^p (2\pi e)^{p/2} / \sqrt{\pi})^{q/p} \\ &\leq \lambda^{(p+q)/p} \times (2R\sqrt{2\pi e} e^{\omega(f, \mathcal{K})+1/6})^q (a_1 p)^{(p+1)/2} (2a_1^{(p+1)/2} p)^{q/p}.\end{aligned}$$

Therefore

$$\begin{aligned}\int_{\mathbb{S}_{p-1}} I_1(\theta) d\theta &\leq \omega_{p-1} \sup_{\theta \in \mathbb{S}_{p-1}} I_1(\theta) \\ &\leq \lambda^{(p+q)/p} \times \frac{2\pi^{p/2}}{\Gamma(p/2)} (2R\sqrt{2\pi e} e^{\omega(f, \mathcal{K})+1/6})^q (a_1 p)^{(p+1)/2} (2a_1^{(p+1)/2} p)^{q/p} \\ &\leq \lambda^{(p+q)/p} p^{(p+q)/p} \times \frac{(2\pi e)^{p/2}}{\sqrt{\pi}} a_1^{(p+1)(p+q)/2p} (4\sqrt{\pi} e^{\omega(f, \mathcal{K})+2/3} R)^q \\ &\leq \lambda^{(p+q)/p} a_3^{p+q} p^{(p+q)/p}\end{aligned}$$

where $a_3 = \max(1, a_1) 4\sqrt{2\pi} e^{\omega(f, \mathcal{K})+7/6} R$.

Note that $F_\lambda(R(\theta)|\theta) < F(R(\theta)|\theta) \leq R^p e^{-l} / (pZ)$ and we also have $Z \geq e^{-u} r^p V_p \geq e^{-u} r^p (2\pi e)^{p/2} / (\sqrt{2\pi} p^{(p+1)/2})$,

then it holds that,

$$\begin{aligned}
I_2(\theta) &\leq \lambda^q \left| F_\lambda(R(\theta)|\theta) \cdot \frac{3\sqrt{\pi}pe^{-l}\text{Vol}(\mathcal{K})}{rc_1^{1/2}Z} + (a_1p)^{(p+1)/2} \int_{C_\epsilon(p)\lambda}^{F_\lambda(R(\theta)|\theta)} \left| \frac{dF^{-1}(z|\theta)}{dz} \right|_{z=\xi} dy \right|^q \\
&\leq \lambda^q \left| \frac{3\sqrt{\pi}R^p e^{-2l}\text{Vol}(\mathcal{K})}{rc_1^{1/2}Z^2} + (a_1p)^{(p+1)/2} \int_{C_\epsilon(p)\lambda}^{F_\lambda(R(\theta)|\theta)} \left| \frac{dF^{-1}(z|\theta)}{dz} \right|_{z=\xi} dy \right|^q \\
&\leq \lambda^q \left| \frac{3\sqrt{\pi}R^p e^{2\omega(f,\mathcal{K})}}{rp+1c_1^{1/2}V_p} + (a_1p)^{(p+1)/2} \int_{C_\epsilon(p)\lambda}^{F_\lambda(R(\theta)|\theta)} \left| \frac{dF^{-1}(z|\theta)}{dz} \right|_{z=\xi} dy \right|^q \\
&\leq \lambda^q \left| \frac{3\sqrt{2}\pi R^p e^{2\omega(f,\mathcal{K})}}{rp+1c_1^{1/2}(2\pi e)^{p/2}} p^{(p+1)/2} + (a_1p)^{(p+1)/2} \int_{C_\epsilon(p)\lambda}^{F_\lambda(R(\theta)|\theta)} \left| \frac{dF^{-1}(z|\theta)}{dz} \right|_{z=\xi} dy \right|^q \\
&\leq \lambda^q (a_4p)^{(p+1)q/2} \int_{C_\epsilon(p)\lambda}^{F_\lambda(R(\theta)|\theta)} \left| \frac{dF^{-1}(z|\theta)}{dz} \right|_{z=\xi} dy
\end{aligned}$$

where $a_4 = 3\sqrt{2}\pi(R/r)e^{2\omega(f,\mathcal{K})}/\min(R\sqrt{c_1}, 1) + a_1$, and $\xi \in [\min\{y \cdot Z_\lambda/Z, y - \epsilon(\theta)\}, \max\{y \cdot Z_\lambda/Z, y - \epsilon(\theta)\}]$. Taking the derivative of F^{-1} gives

$$\frac{dF^{-1}(z|\theta)}{dz} = \frac{1}{F'(F^{-1}(z|\theta)|\theta)} = \frac{Ze^{f(F^{-1}(z|\theta)\theta)}}{F^{-1}(z|\theta)^{p-1}}.$$

Recall that $f(x) \leq u$ on \mathcal{K} . Notice that $F^{-1}(z|\theta) \leq R(\theta)$ since

$$z \leq \max\{F_\lambda(R(\theta)|\theta) \cdot Z_\lambda/Z, F_\lambda(R(\theta)|\theta) - \epsilon(\theta)\} \leq F(R(\theta)|\theta),$$

By the monotonicity of F , this implies $F^{-1}(z|\theta) \leq R(\theta)$. Consequently, since $f(x) \leq u$ for all $x \in \mathcal{K}$, it follows that

$$e^{f(F^{-1}(z|\theta)\theta)} \leq e^u.$$

Moreover, we have $\xi \geq \min\{y \cdot Z_\lambda/Z, y - \epsilon(\theta)\} \geq y/2$. Therefore, by Lemma 9, it follows that

$$\left| \frac{dF^{-1}(z|\theta)}{dz} \right|_{z=\xi} \leq \left| \frac{Ze^u}{[z^{1/p}(pZe^l)^{1/p}]^{p-1}} \right|_{z=\xi} \leq \frac{2^{(p-1)/p}Ze^u}{(pZe^l)^{(p-1)/p}} \cdot y^{1/p-1}$$

Substitute it into the upper bound of $\phi_2(t)$, then it holds that

$$I_2(\theta) \leq \lambda^q (a_4p)^{(p+1)q/2} \left(\frac{2Z^{1/p}e^u}{(pel)^{(p-1)/p}} \right)^q \int_{C_\epsilon(p)\lambda}^{F_\lambda(R(\theta)|\theta)} y^{q/p-q} dy.$$

If $1/p + 1/q > 1$, then

$$\begin{aligned}
I_2(\theta) &\leq \lambda^q (a_4p)^{(p+1)q/2} \left(\frac{2Z^{1/p}e^u}{(pel)^{(p-1)/p}} \right)^q \frac{F(R(\theta)|\theta)^{q(1/p+1/q-1)}}{q(1/p+1/q-1)} \\
&\leq \lambda^q (a_4p)^{(p+1)q/2} p/q \left(\frac{2Z^{1/p}e^u}{(pel)^{(p-1)/p}} \right)^q \left(\frac{e^{-l}R^p}{pZ} \right)^{q(1/p+1/q-1)} \\
&\leq \lambda^q (a_4p)^{(p+1)q/2} 2^q e^{qu-l} Z^{q-1} R^{p+q-pq} \\
&\leq \lambda^q (a_4p)^{(p+1)q/2} (2R)^q e^{q\omega(f,\mathcal{K})+1/6(q-1)} \times \frac{(2\pi e)^{p(q-1)/2}}{(\sqrt{\pi}p^{(p+1)/2})^{q-1}} \\
&\leq \lambda^q (a_5p)^{(p+1)/2},
\end{aligned}$$

where $a_5 = (4\pi a_4 e^{\omega(f,\mathcal{K})+7/6})^q \max(R, 1)^q$.

If $1/p + 1/q = 1$, then $p = q = 2$, and $\phi_2(\theta) = \tilde{\mathcal{O}}(\lambda^q)$. If $1/p + 1/q < 1$, then

$$\begin{aligned} I_2(\theta) &\leq \lambda^q (a_4 p)^{(p+1)q/2} \left(\frac{2Z^{1/p} e^u}{(pe^l)^{(p-1)/p}} \right)^q \frac{(C_\epsilon(p)\lambda)^{q(1/p+1/q-1)}}{q(1-1/p-1/q)} \\ &\leq \lambda^{(p+q)/p} (a_4 p)^{(p+1)q/2} \frac{3 \times (2e^{\omega(f,\mathcal{K})+1/6} R(2\pi e))^q}{q\pi^{q/2}} \times \frac{(a_1 p)^{(p+1)q(1/p+1/q-1)/2}}{p^{[(p+1)/2p+(p-1)/p]q}} \\ &\leq \lambda^{(p+q)/p} a_6^{(p+1)/2} p^{(p+1)/2-(p-1)q/p} \end{aligned}$$

where $a_6 = (12a_4 e^{\omega(f,\mathcal{K})+1/6})^q \max(R, 1)^q / \min(a_1, 1)^q$. Therefore, we obtain that

$$\begin{aligned} \int_{\mathbb{S}_{p-1}} \phi_2(\theta) d\theta &\leq \lambda^{(p+q)/p} a_3^{p+q} p^{(p+q)/p} + \omega_{p-1} \sup_{\theta \in \mathbb{S}_{p-1}} I_2(\theta) \\ &\leq \lambda^{(p+q)/p} a_3^{p+q} p^{(p+q)/p} + \frac{(2\pi e)^{p/2}}{\sqrt{\pi}} p^{-(p-1)/2} \sup_{\theta \in \mathbb{S}_{p-1}} I_2(\theta) \\ &\leq a_7^{p+q} p^{(p+q)/p} \lambda^{q\alpha} \end{aligned}$$

where $a_7 = \max(a_3, a_5, a_6, 1)$ and $\alpha = \min(1/p + 1/q, 1)$. Here we omit the logarithmic factor of λ . Therefore, we arrive at

$$\int_{\mathbb{S}_{p-1}} \phi_2(\theta) d\theta = \begin{cases} \mathcal{O}(\lambda^q), & 1/p + 1/q > 1 \\ \mathcal{O}(\lambda^q \log(\frac{1}{\lambda})), & 1/p + 1/q = 1 \\ \mathcal{O}(\lambda^{q(1/p+1/q)}), & 1/p + 1/q < 1 \end{cases}$$

Step 3. To establish the upper bound for ϕ_3 , we need the following lemma.

Lemma 10. Define the set $\mathcal{K}_t := \{x \in \mathbb{R}^p : \|x - \mathbb{P}_{\mathcal{K}}(x)\|_2 \leq t\}$. It holds for any $t > 0$ that $\mathcal{K}_t \subset (1+t/r)\mathcal{K}$. Moreover, under Assumption 3, it implies that

$$\|x - \mathbb{P}_{\mathcal{K}}(x)\|_2^2 \geq r^2(g_{\mathcal{K}}(x) - 1)^2$$

where $g_{\mathcal{K}}$ is the variation of Gauge function defined in Example 2.2.

By Lemma 10, it follows that

$$\mathcal{K}_t \subset \left(1 + \frac{t}{r}\right)\mathcal{K}.$$

In particular, this implies that for any $x \in \mathbb{R}^p$,

$$x \in \left(1 + \frac{\|x - \mathbb{P}_{\mathcal{K}}(x)\|_2}{r}\right)\mathcal{K}.$$

Therefore, for any $x = t\theta \in \mathcal{K}^c$, we have

$$t - R(\theta) \leq \left(1 + \frac{\|x - \mathbb{P}_{\mathcal{K}}(x)\|_2}{r}\right)R(\theta) - R(\theta) = \frac{\|x - \mathbb{P}_{\mathcal{K}}(x)\|_2}{r}R(\theta)$$

Using the inequality that $(a + b)^q \leq 2^{q-1}(a^q + b^q)$ and Assumption 3, we have

$$\begin{aligned}\phi_3(\theta) &= \int_{R(\theta)}^{\infty} |t - g(F_{\lambda}(t, \theta) - \epsilon(\theta), \theta)|^q \frac{e^{-f(t\theta) - \frac{1}{2\lambda^2}d_{\mathcal{K}}(t\theta)}}{Z_{\lambda}} dt \\ &\leq \int_{R(\theta)}^{\infty} |t - R(\theta) + R(\theta) - g(F_{\lambda}(t, \theta) - \epsilon(\theta), \theta)|^q \frac{e^{-f(t\theta) - \frac{c_1}{2\lambda^2}\|t\theta - P_{\mathcal{K}}(t\theta)\|_2^2}}{Z_{\lambda}} dt \\ &\leq \int_{R(\theta)}^{\infty} |t - R(\theta) + R(\theta) - g(F_{\lambda}(t, \theta) - \epsilon(\theta), \theta)|^q \frac{e^{-f(t\theta) - \frac{c_1 r^2}{2\lambda^2 R(\theta)^2}(t-R(\theta))^2}}{Z_{\lambda}} dt\end{aligned}$$

Recall the definition of $\epsilon(\theta)$, and observe that for any $t \geq R(\theta)$,

$$\begin{aligned}R(\theta) - g(F_{\lambda}(t, \theta) - \epsilon(\theta), \theta) &\leq R(\theta) - g(F_{\lambda}(R(\theta), \theta) - \epsilon(\theta), \theta) \\ &= F^{-1}(F(R(\theta)|\theta)|\theta) - F^{-1}(F(R(\theta)|\theta) - \delta(\theta)|\theta) \\ &= \delta(\theta) \cdot \left. \frac{dF^{-1}(z)}{dz} \right|_{z=\xi}\end{aligned}$$

where $\delta(\theta) = F_{\lambda}(\infty, \theta) - F_{\lambda}(R(\theta), \theta)$, then

$$\delta(\theta) \leq \frac{1}{Z} \int_{R(\theta)}^{\infty} t^{p-1} e^{-f(t\theta) - \frac{1}{2\lambda^2}d_{\mathcal{K}}(t\theta)} dt \leq (a_1 p)^{(p+1)/2} \lambda.$$

where we use the same argument in the proof of Lemma 8. In addition,

$$\begin{aligned}\left. \frac{dF^{-1}(z)}{dz} \right|_{z=\xi} &\leq \left. \frac{Ze^u}{[z^{1/p}(pZe^l)^{1/p}]^{p-1}} \right|_{z=\xi} \\ &\leq \frac{2Ze^u}{F(R(\theta)|\theta)^{(p-1)/p}(pZe^l)^{(p-1)/p}} \\ &\leq \frac{2Ze^u e^{\omega(f, \mathcal{K})}}{r^{p-1}} \\ &\leq \frac{2e^{2\omega(f, \mathcal{K})+1/6} R^p (2\pi e)^{p/2}}{r^{p-1}} p^{-(p+1)/2}\end{aligned}$$

Therefore

$$R(\theta) - g(F_{\lambda}(t, \theta) - \epsilon(\theta), \theta) \leq a_8^{(p+1)/2} \lambda,$$

where $a_8 = 4\pi a_1 e^{2\omega(f, \mathcal{K})+7/6} \max(1, R^2) / \min(1, r^2)$. Thus, we obtain that

$$\begin{aligned}\phi_3(\theta) &\leq e^{-l} \int_{R(\theta)}^{\infty} |t - R(\theta) + a_8^{(p+1)/2} \lambda|^q \frac{e^{-\frac{c_1 r^2}{2\lambda^2 R(\theta)^2}(t-R(\theta))^2}}{Z} dt \\ &\leq \frac{e^{-l} \lambda}{Z} \int_0^{\infty} |\lambda s + a_8^{(p+1)/2} \lambda|^q e^{-\frac{c_1 r^2}{2R(\theta)^2}s^2} ds \\ &= \frac{e^{-l}}{Z} \cdot \lambda^{q+1} \int_0^{\infty} |s + a_8^{(p+1)/2}|^q e^{-\frac{c_1 r^2}{2R(\theta)^2}s^2} ds \\ &\leq \frac{\sqrt{2\pi} e^{\omega(f, \mathcal{K})} p^{(p+1)/2}}{r^p (2\pi e)^{p/2}} \times 2^{q-1} \left(\frac{1}{2} \frac{(2R^2)^{(q+1)/2}}{(c_1 r^2)^{(q+1)/2}} \Gamma\left(\frac{q+1}{2}\right) + \frac{1}{2} a_8^{(p+1)q/2} \sqrt{\frac{2\pi R^2}{c_1 r^2}} \right) \\ &\leq a_9^{(p+1)/2} p^{(p+1)/2} \lambda^{q+1}.\end{aligned}$$

Thus,

$$\int_{\mathbb{S}_{p-1}} \phi_3(\theta) d\theta \leq a_{10}^{(p+1)/2} p \lambda^{q+1}.$$

Combining all the upper bounds of $\phi_i(\theta), i = 1, 2, 3$ we find

$$W_q^q(\nu, T_\#(\nu^\lambda)) \leq \max(a_2 + a_7 + a_{10}, 1)^{p+q} p^{(p+q)/p} \cdot \begin{cases} \lambda^q, & 1/p + 1/q > 1 \\ \lambda^q \log(\frac{1}{\lambda}), & 1/p + 1/q = 1 \\ \lambda^{q(1/p+1/q)}, & 1/p + 1/q < 1. \end{cases}$$

Recalling that $W_q^q(\nu, T_\#(\nu^\lambda)) \leq a_2^{p+q} p^{(p+q)/p} \lambda^{(p+q)/p}$, we arrive at the desired result

$$W_q(\nu, \nu^\lambda) = C(p, q) \cdot \begin{cases} \lambda, & 1/p + 1/q > 1 \\ \lambda \log(\frac{1}{\lambda})^{1/q}, & 1/p + 1/q = 1 \\ \lambda^{1/p+1/q}, & 1/p + 1/q < 1. \end{cases}$$

where $C(p, q) = \max(2a_2 + a_7 + a_{10}, 1)^{(p+q)/q} p^{1/p+1/q}$.

□

B.2 Proof of Proposition 2

Assume f is M -smooth and d_K is M_0 -smooth. To prove Proposition 2, we need the following auxiliary lemma.

Lemma 11. *Under the assumptions stated in Proposition 2, for any $k \geq 1$, when $\lambda = o(r/p)$, it holds that*

$$\int_{K^c} \|x\|_2^k \nu^\lambda(dx) / \mu_k(\nu) \geq \frac{\tilde{C}(c_1, c_2, M_0, M, K) r^{p+k-1} (k+p)}{2\omega_{p-1} R^{k+p}} \lambda.$$

where $\tilde{C}(c_1, c_2, M_0, M, K)$ is a constant independent of r and p, k .

We are now ready to prove Proposition 2.

Proof. [Proof of Proposition 2] Define

$$\rho_1 := \frac{\int_K \|x\|_2^q e^{-f(x)} dx}{\int_K e^{-f(x)} dx}, \quad \rho_2(\lambda) := \frac{\int_{K^c} \|x\|_2^q e^{-f(x) - \frac{1}{2\lambda^2} d_K(x)} dx}{\int_{K^c} e^{-f(x) - \frac{1}{2\lambda^2} d_K(x)} dx}.$$

Then

$$\int_{\mathbb{R}^p} \|x\|_2^q \nu^\lambda(dx) = \frac{\rho_1 \int_K e^{-f(x)} dx + \rho_2(\lambda) \int_{K^c} e^{-f(x) - \frac{1}{2\lambda^2} d_K(x)} dx}{\int_K e^{-f(x)} dx + \int_{K^c} e^{-f(x) - \frac{1}{2\lambda^2} d_K(x)} dx}, \quad \int_{\mathbb{R}^p} \|x\|_2^q \nu(dx) = \rho_1.$$

By Proposition 7.29 in [Vil09], it holds for any $q \geq 1$ that

$$W_q(\nu^\lambda, \nu) \geq \left| \left(\int_{\mathbb{R}^p} \|x\|_2^q \nu^\lambda(dx) \right)^{1/q} - \left(\int_{\mathbb{R}^p} \|x\|_2^q \nu(dx) \right)^{1/q} \right|.$$

Note that when $|\delta| < \frac{1}{3}$, it holds that $|(1 + \delta)^{1/k} - 1| > \frac{1}{2k}|\delta|$. Therefore, if we denote

$$\delta := \frac{\int_{\mathbb{R}^p} \|x\|_2^q \nu^\lambda(dx)}{\int_{\mathbb{R}^p} \|x\|_2^q \nu(dx)} - 1,$$

then we obtain that

$$\begin{aligned} W_q(\nu^\lambda, \nu) &\geq \frac{1}{2q} \left(\int_{\mathbb{R}^p} \|x\|_2^q \nu(dx) \right)^{1/q} |\delta| \\ &= \frac{1}{2q} \left(\int_{\mathbb{R}^p} \|x\|_2^q \nu(dx) \right)^{1/q-1} \left| \int_{\mathbb{R}^p} \|x\|_2^q \nu^\lambda(dx) - \int_{\mathbb{R}^p} \|x\|_2^q \nu(dx) \right|. \end{aligned}$$

Therefore, it is enough to show the last term is $\Omega(\lambda)$.

$$\left| \int_{\mathbb{R}^p} \|x\|_2^q \nu^\lambda(dx) - \int_{\mathbb{R}^p} \|x\|_2^q \nu(dx) \right| = \frac{\int_{\mathcal{K}^c} e^{-f(x) - \frac{1}{2\lambda^2} d_{\mathcal{K}}(x)} dx}{\int_{\mathcal{K}} e^{-f(x)} dx + \int_{\mathcal{K}^c} e^{-f(x) - \frac{1}{2\lambda^2} d_{\mathcal{K}}(x)} dx} \cdot |\rho_2(\lambda) - \rho_1|.$$

By Lemma 11, the first term on the right side is $\Omega(\lambda)$, then it remains to show $|\rho_2(\lambda) - \rho_1| = \Omega(1)$. To prove this, we derive the limit of $\rho_2(\lambda)$ when λ approaches zero, and the desired result follows by the condition.

For Case 1 with $Q = I$, $d_{\mathcal{K}}(x) = \|x - \mathbf{P}_{\mathcal{K}}(x)\|_2^2 = \text{dist}(x, \mathcal{K})^2$. We assume that \mathcal{K} has a C^2 -boundary, then it holds for any $\varepsilon > 0$ that

$$\begin{aligned} &\lim_{\lambda \rightarrow 0} \frac{1}{\lambda} \int_{\mathcal{K}^c} \|x\|_2^q e^{-f(x) - \frac{1}{2\lambda^2} d_{\mathcal{K}}(x)} dx \\ &= \lim_{\lambda \rightarrow 0} \frac{1}{\lambda} \int_{\bar{\mathcal{K}}_\varepsilon - \mathcal{K}} \|x\|_2^q e^{-f(x) - \frac{1}{2\lambda^2} \text{dist}(x, \mathcal{K})^2} dx + \lim_{\lambda \rightarrow 0} \frac{1}{\lambda} \int_{\bar{\mathcal{K}}_\varepsilon^c} \|x\|_2^q e^{-f(x) - \frac{1}{2\lambda^2} \text{dist}(x, \mathcal{K})^2} dx \\ &= \lim_{\lambda \rightarrow 0} \frac{1}{\lambda} \int_{\bar{\mathcal{K}}_\varepsilon - \mathcal{K}} \|x\|_2^q e^{-f(x) - \frac{1}{2\lambda^2} \text{dist}(x, \mathcal{K})^2} dx. \end{aligned}$$

where $\bar{\mathcal{K}}_\varepsilon := \{x \in \mathbb{R}^p : \text{dist}(x, \mathcal{K}) \leq \varepsilon\}$, the last equality follows from Dominated Convergence Theorem (DCT). To evaluate the integral $I = \int_{\bar{\mathcal{K}}_\varepsilon - \mathcal{K}} \|x\|_2^q e^{-f(x) - \frac{1}{2\lambda^2} \text{dist}(x, \mathcal{K})^2} dx$, we utilize a tubular neighborhood parameterization. The diffeomorphism $\Phi : \partial\mathcal{K} \times (0, \varepsilon) \rightarrow \mathcal{K}^c$, defined as $x = z + tv(z)$, uniquely maps points near $\partial\mathcal{K}$ to coordinates (z, t) , where $z \in \partial\mathcal{K}$ and $t = \text{dist}(x, \mathcal{K})$. The Jacobian determinant $J(z, t)$, accounting for curvature effects, is $\prod_{i=1}^{p-1} (1 - t\kappa_i(z))$, with $\kappa_i(z)$ as principal curvatures. Thus

$$\begin{aligned} \lim_{\lambda \rightarrow 0} \frac{1}{\lambda} I &= \lim_{\lambda \rightarrow 0} \frac{1}{\lambda} \int_{\partial\mathcal{K}} \int_0^\varepsilon \|z + tv(z)\|_2^q e^{-f(z+tv(z))} J(z, t) e^{-\frac{t^2}{2\lambda^2}} dt d\sigma(z) \\ &= \lim_{\lambda \rightarrow 0} \frac{1}{\lambda} \int_{\partial\mathcal{K}} \int_0^\infty \|z + tv(z)\|_2^q e^{-f(z+tv(z))} J(z, t) e^{-\frac{t^2}{2\lambda^2}} dt d\sigma(z). \end{aligned}$$

where $J(z, t) := 1$ if $t > \varepsilon$, the second equality follows from DCT. After parameterizing $x = z + tv(z)$, a substitution for t can further simplify the radial integral. Defining $s = t/\lambda$, the integral becomes

$$\begin{aligned} \lim_{\lambda \rightarrow 0} \frac{1}{\lambda} I &= \lim_{\lambda \rightarrow 0} \int_{\partial\mathcal{K}} \int_0^\infty \|z + \lambda sv(z)\|_2^q e^{-f(z+\lambda sv(z))} J(z, \lambda s) e^{-\frac{s^2}{2}} ds d\sigma(z) \\ &= \int_{\partial\mathcal{K}} \int_0^\infty \|z\|_2^q e^{-f(z)} e^{-\frac{s^2}{2}} ds d\sigma(z) \\ &= \sqrt{\frac{\pi}{2}} \int_{\partial\mathcal{K}} \|z\|_2^q e^{-f(z)} d\sigma(z). \end{aligned}$$

Similarly, we obtain that

$$\lim_{\lambda \rightarrow 0} \frac{1}{\lambda} \int_{\mathcal{K}^c} e^{-f(x) - \frac{1}{2\lambda^2} d_{\mathcal{K}}(x)} dx = \sqrt{\frac{\pi}{2}} \int_{\partial\mathcal{K}} e^{-f(z)} d\sigma(z).$$

Therefore,

$$\lim_{\lambda \rightarrow 0} \rho_2(\lambda) = \frac{\int_{\partial\mathcal{K}} \|z\|_2^q e^{-f(z)} d\sigma(z)}{\int_{\partial\mathcal{K}} e^{-f(z)} d\sigma(z)}.$$

For Case 2, we employ a parameterization aligned with the geometric interpretation of the Gauge function. For $x \in \mathcal{K}^c$, the Gauge function $\gamma_{\mathcal{K}}(x)$ defines the minimal scaling factor $s \geq 1$ such that $x = sz$ for some $z \in \partial\mathcal{K}$. This allows the parameterization $x = (1+t)z$, where $t > 0$ and $z \in \partial\mathcal{K}$, ensuring $\gamma_{\mathcal{K}}(x) = 1+t$. The volume element dx transforms under this radial scaling as $dx = (1+t)^{p-1} d\sigma(z) dt$, therefore,

$$\begin{aligned} & \lim_{\lambda \rightarrow 0} \frac{1}{\lambda} \int_{\mathcal{K}^c} \|x\|_2^q e^{-f(x) - \frac{1}{2\lambda^2} d_{\mathcal{K}}(x)} dx \\ &= \lim_{\lambda \rightarrow 0} \frac{1}{\lambda} \int_{\partial\mathcal{K}} \int_0^\infty \|(1+t)z\|_2^q e^{-f((1+t)z)} e^{-\frac{t^2}{2\lambda^2}} (1+t)^{p-1} dt d\sigma(z) \\ &= \lim_{\lambda \rightarrow 0} \int_{\partial\mathcal{K}} \int_0^\infty \|(1+\lambda s)z\|_2^k e^{-f((1+\lambda s)z)} e^{-\frac{s^2}{2}} (1+\lambda s)^{p-1} ds d\sigma(z) \\ &= \sqrt{\frac{\pi}{2}} \int_{\partial\mathcal{K}} \|z\|_2^q e^{-f(z)} d\sigma(z). \end{aligned}$$

The last equality follows from DCT, and similarly we obtain that

$$\lim_{\lambda \rightarrow 0} \rho_2(\lambda) = \frac{\int_{\partial\mathcal{K}} \|z\|_2^q e^{-f(z)} d\sigma(z)}{\int_{\partial\mathcal{K}} e^{-f(z)} d\sigma(z)}.$$

which is the same as Case 1. \square

B.3 Proof of Auxiliary Lemmas

Proof. [Proof of Lemma 7] By Assumption 3, we have

$$\int_{\mathcal{K}^c} \|x\|_2^k e^{-U^\lambda(x)} dx = \int_{\mathcal{K}^c} \|x\|_2^k e^{-f(x)} \cdot e^{-\frac{1}{2\lambda^2} d_{\mathcal{K}}(x)} dx \leq \int_{\mathcal{K}^c} \|x\|_2^k e^{-f(x)} \cdot e^{-\frac{c_1}{2\lambda^2} \|x - \mathbb{P}_{\mathcal{K}}(x)\|_2^\alpha}.$$

By Fubini's theorem and the fact that

$$\int_0^\infty \frac{c_1 t}{\lambda^2} e^{-\frac{c_1 t^2}{2\lambda^2}} \mathbf{1}_{[\|x - \mathbb{P}_{\mathcal{K}}(x)\|_2, +\infty)}(t) dt = e^{-\frac{c_1}{2\lambda^2} \|x - \mathbb{P}_{\mathcal{K}}(x)\|_2^2},$$

it holds for every $k \geq 0$ that

$$\int_{\mathcal{K}^c} \|x\|_2^k e^{-U^\lambda(x)} dx \leq \int_0^\infty \underbrace{\left(\int_{\mathcal{K}^c} \|x\|_2^k e^{-f(x)} \mathbf{1}_{(\|x - \mathbb{P}_{\mathcal{K}}(x)\|_2 \leq t)} dx \right)}_{\psi(t)} \frac{c_1 t}{\lambda^2} e^{-\frac{c_1 t^2}{2\lambda^2}} dt. \quad (\text{B.4})$$

Then we focus on $\psi(t)$, that is

$$\begin{aligned}\psi(t) &\leq e^{-l} \int_{\mathcal{K}^c} \|x\|_2^k \mathbf{1}(\|x - \mathbb{P}_{\mathcal{K}}(x)\|_2 \leq t) dx \\ &= e^{-l} \left(\int_{\mathcal{K}_t} \|x\|_2^k dx - \int_{\mathcal{K}} \|x\|_2^k dx \right) \\ &\leq e^{-l} \left(\int_{(1+t/r)\mathcal{K}} \|x\|_2^k dx - \int_{\mathcal{K}} \|x\|_2^k dx \right).\end{aligned}$$

where l is the lower bound of f in \mathbb{R}^p . The last inequality use the fact that $\mathcal{K} \subset \mathcal{K}_t/(1+t/r)$ proved in Lemma 10. Therefore we have

$$\psi(t) \leq e^{-l} \left[(1+t/r)^{p+k} - 1 \right] \int_{\mathcal{K}} \|x\|_2^k dx \leq e^{-l} \cdot \left(e^{(p+k)t/r} - 1 \right) \int_{\mathcal{K}} \|x\|_2^k dx.$$

Substituting this upper bound in (B.4) leads to

$$\int_{\mathcal{K}^c} \|x\|_2^k e^{-U^\lambda(x)} dx \leq \underbrace{\int_0^\infty \frac{c_1 t}{\lambda^2} e^{-\frac{c_1 t^2}{2\lambda^2}} (e^{(p+k)t/r} - 1) dt}_{I} \times e^{-l} \int_{\mathcal{K}} \|x\|_2^k dx$$

Next, we derive a closed-form upper bound for the integral term,

$$\begin{aligned}I &= \int_0^\infty \frac{c_1 t}{\lambda^2} e^{-\frac{c_1 t^2}{2\lambda^2}} (e^{(p+k)t/r} - 1) dt \\ &= \int_0^\infty (e^{(p+k)t/r} - 1) d\left(-e^{-c_1 t^2/2\lambda^2}\right) \\ &= \frac{p+k}{r} \int_0^\infty \exp\left\{-\frac{c_1 t^2}{2\lambda^2} + \frac{(p+k)t}{r}\right\} dt.\end{aligned}$$

By Young's inequality, we have

$$\frac{(p+k)t}{r} \leq \frac{\eta t^2}{2} + \frac{(p+k)^2}{2r^2\eta}, \quad \eta > 0$$

Setting $\eta = \frac{c_1}{2\lambda^2}$ and combining this with the previous displays, we obtain

$$\begin{aligned}I &\leq \frac{p+k}{r} \exp\left(\frac{\lambda^2(p+k)^2}{c_1 r^2}\right) \int_0^\infty \exp\left(-\frac{c_1 t^2}{4\lambda^2}\right) dt \\ &\leq \frac{(p+k)\Gamma(3/2)}{r} \left(\frac{4\lambda^2}{c_1}\right)^{1/2} \exp\left(\frac{\lambda^2(p+k)^2}{c_1 r^2}\right).\end{aligned}$$

When $\lambda < c_1^{1/2}r/(p+k)$, it follows that

$$\int_{\mathcal{K}^c} \|x\|_2^k e^{-U^\lambda(x)} dx \leq \frac{3\sqrt{\pi}(p+k)}{rc_1^{1/2}} \lambda \times e^{-l} \int_{\mathcal{K}} \|x\|_2^k dx.$$

□

Proof. [Proof of Lemma 8] By rearranging the term and the triangle inequality, we have

$$\begin{aligned} |\epsilon(\theta)| &= \left| \frac{\int_0^{R(\theta)} t^{p-1} e^{-f(t\theta)} dt + \int_{R(\theta)}^\infty t^{p-1} e^{-f(t\theta) - \frac{1}{2\lambda^2} d_{\mathcal{K}}(t\theta)} dt}{Z_\lambda} - \frac{\int_0^{R(\theta)} t^{p-1} e^{-f(t\theta)} dt}{Z} \right| \\ &\leq \left| \frac{1}{Z_\lambda} - \frac{1}{Z} \right| \cdot \int_0^{R(\theta)} t^{p-1} e^{-f(t\theta)} dt + \frac{1}{Z_\lambda} \int_{R(\theta)}^\infty t^{p-1} e^{-f(t\theta) - \frac{1}{2\lambda^2} d_{\mathcal{K}}(t\theta)} dt \times \end{aligned}$$

Recall the display (B.1), then we have

$$\begin{aligned} |\epsilon(\theta)| &\leq \int_0^{R(\theta)} t^{p-1} e^{-f(t\theta)} dt \times \frac{Z_\lambda - Z}{Z^2} + \int_{R(\theta)}^\infty t^{p-1} e^{-f(t\theta) - \frac{1}{2\lambda^2} d_{\mathcal{K}}(t\theta)} dt \times \frac{1}{Z} \\ &\leq \int_0^R t^{p-1} e^{-l} dt \times \frac{3\sqrt{\pi} p e^{-l} \text{Vol}(\mathcal{K})}{r c_1^{1/2} Z^2} \lambda + \frac{e^{-l}}{Z} \int_{R(\theta)}^\infty t^{p-1} e^{-\frac{c_1 r^2}{2\lambda^2} \|t\theta - \mathbf{P}_{\mathcal{K}}(t\theta)\|_2^2} dt \\ &\leq \frac{3\sqrt{\pi} R^p e^{-2l} \text{Vol}(\mathcal{K})}{r c_1^{1/2} Z^2} \lambda + \frac{e^{-l}}{Z} \underbrace{\int_{R(\theta)}^\infty t^{p-1} e^{-\frac{c_1 r^2}{2\lambda^2 R(\theta)^2} (t - R(\theta))^2} dt}_{I(\theta)}. \end{aligned}$$

The last inequality follows from Lemma 10, since $g_{\mathcal{K}}(t\theta) = [t - R(\theta)]/R(\theta)$. Substitute $s = [t - R(\theta)]/\lambda$,

$$\begin{aligned} I(\theta) &= \lambda \times \int_0^\infty (R(\theta) + \lambda s)^{p-1} e^{-\frac{c_1 r^2}{2R(\theta)^2} s^2} ds \\ &\leq \lambda \times \int_0^\infty (R + \lambda s)^{p-1} e^{-\frac{c_1 r^2}{2R^2} s^2} ds \\ &\leq \lambda \times 2^{p-2} \left(\frac{\sqrt{\pi} R^{p-1}}{2\sqrt{c_1 r^2 / 2R^2}} + \frac{\lambda^{p-1} \Gamma(p/2)}{2(c_1 r^2 / 2R^2)^{p/2}} \right) \end{aligned}$$

Therefore, we have

$$|\epsilon(\theta)| \leq \left[\frac{3\sqrt{\pi} R^p e^{-2l} \text{Vol}(\mathcal{K})}{r c_1^{1/2} Z^2} + \frac{2^{p-2} e^{-l}}{Z} \left(\frac{\sqrt{\pi} R^{p-1}}{2\sqrt{c_1 r^2 / 2R^2}} + \frac{\lambda^{p-1} \Gamma(p/2)}{2(c_1 r^2 / 2R^2)^{p/2}} \right) \right] \lambda,$$

where the coefficient is independent of θ . Note that $e^{-u} \text{Vol}(\mathcal{K}) \leq Z \leq e^{-l} \text{Vol}(\mathcal{K})$ and $r^p V_p \leq \text{Vol}(\mathcal{K}) \leq R^p V_p$, and we have

$$\frac{1}{\sqrt{2\pi}} \cdot \frac{(2\pi e)^{p/2}}{p^{(p+1)/2}} \leq V_p \leq \frac{e^{1/6}}{\sqrt{\pi}} \cdot \frac{(2\pi e)^{p/2}}{p^{(p+1)/2}}, \quad \frac{2\sqrt{\pi} p^{(p-1)/2}}{(2e)^{p/2}} \leq \Gamma\left(\frac{p}{2}\right) \leq \frac{2\sqrt{\pi} e^{1/6} p^{(p-1)/2}}{(2e)^{p/2}}.$$

Thus when $\lambda = o(r/p)$, we obtain that $|\epsilon(\theta)| \leq C_\epsilon(p)\lambda$, where

$$\begin{aligned}
C_\epsilon(p) &= \frac{3\sqrt{\pi}R^p e^{2\omega(f,\mathcal{K})}R^p}{rc_1^{1/2}r^p} \cdot \frac{\sqrt{2\pi}p^{(p+1)/2}}{(2\pi e)^{p/2}} + \frac{\pi 2^{p-2}e^{\omega(f,\mathcal{K})}p^{(p+1)/2}}{r^p(2\pi e)^{p/2}} \cdot \frac{R^p}{c_1^{1/2}r} \\
&\quad + \frac{2^{p-2}e^{\omega(f,\mathcal{K})}p^{(p+1)/2}}{r^p(2\pi e)^{p/2}} \cdot \frac{\sqrt{\pi}e^{1/6}R^p}{e^{p/2}c_1^{p/2}r} \\
&= \frac{3\sqrt{\pi}e^{2\omega(f,\mathcal{K})}\sqrt{2\pi}\sqrt{2\pi e}}{c_1^{1/2}R^2} \cdot \left(\frac{pR^4}{(2\pi e)r^2}\right)^{(p+1)/2} + \frac{\pi e^{\omega(f,\mathcal{K})}\sqrt{2\pi e}}{16c_1^{1/2}R} \cdot \left(\frac{2R^2p}{\pi er^2}\right)^{(p+1)/2} \\
&\quad + \frac{\sqrt{2}\pi\sqrt{c_1}e^{\omega(f,\mathcal{K})+7/6}}{8} \cdot \left(\frac{2pR^2}{\pi e^2c_1r^2}\right)^{(p+1)/2}.
\end{aligned}$$

Set

$$a_1 = \max \left\{ \frac{6\sqrt{\pi}e^{2\omega(f,\mathcal{K})-1/2}R^2}{r^2c_1^{1/2}}, \frac{e^{\omega(f,\mathcal{K})}\sqrt{2\pi e}R}{8c_1^{1/2}er^2}, \frac{\sqrt{2}e^{\omega(f,\mathcal{K})-5/6}R^2}{4c_1^{1/2}r^2} \right\}$$

Then $C_\epsilon(p) \leq (a_1 p)^{(p+1)/2}$. \square

Proof. [Proof of Lemma 10] It holds for any $x \in \mathcal{K}_t/(1+b)$ that

$$\|(1+b)x - P_{\mathcal{K}}((1+b)x)\|_2 \leq t$$

which is equivalent to

$$\frac{1+b}{b}\|x - \frac{1}{1+b}P_{\mathcal{K}}((1+b)x)\|_2 \leq \frac{t}{b}.$$

Note that we can rewrite x as

$$x = \frac{1}{1+b}P_{\mathcal{K}}((1+b)x) + \frac{b}{1+b}\frac{x - \frac{1}{1+b}P_{\mathcal{K}}((1+b)x)}{\frac{b}{1+b}}.$$

Notice that

$$P_{\mathcal{K}}((1+b)x) \in \mathcal{K}$$

and when $b = t/r$ we have

$$\frac{x - \frac{1}{1+b}P_{\mathcal{K}}((1+b)x)}{\frac{b}{1+b}} \in \mathcal{K}.$$

By the convexity of the set \mathcal{K} , this implies $x \in \mathcal{K}$, then we obtain that $\mathcal{K}_t \subset (1 + \frac{t}{r})\mathcal{K}$. For the second claim, recall the definition of $g_{\mathcal{K}}$, it holds for any $x \in \mathcal{K}_t$ that $g_{\mathcal{K}}(x) \leq 1 + t/r$. Thus set $t = \|x - P_{\mathcal{K}}(x)\|_2$, then we have

$$g_{\mathcal{K}}(x) \leq 1 + \frac{\|x - P_{\mathcal{K}}(x)\|_2}{r}$$

which reach the desired result. \square

Proof. [Proof of Lemma 11] By the definition of ν^λ and $\mu_k(\nu)$, we have

$$\int_{\mathcal{K}^c} \|x\|_2^k \nu^\lambda(dx) / \mu_k(\nu) = \frac{\int_{\mathcal{K}^c} \|x\|_2^k e^{-f(x) - \frac{1}{2\lambda^2} d_{\mathcal{K}}(x)} dx}{\int_{\mathbb{R}^p} e^{-U^\lambda(x)} dx} \cdot \frac{\int_{\mathcal{K}} e^{-f(x)} dx}{\int_{\mathcal{K}} \|x\|_2^k e^{-f(x)} dx}. \quad (\text{B.5})$$

Note that f is M -smooth, it then holds that

$$f(x) \leq f(0) + \frac{M}{2} \|x\|_2^2.$$

This implies

$$\int_{\mathcal{K}^c} \|x\|_2^k e^{-f(x) - \frac{1}{2\lambda^2} d_{\mathcal{K}}(x)} dx \geq e^{-f(0)} \int_{\mathcal{K}^c} \|x\|_2^k e^{-\frac{M}{2}\|x\|_2^2 - \frac{c_2}{2\lambda^2}\|x - P_{\mathcal{K}}(x)\|_2^2} dx.$$

By Fubini's theorem and the fact that

$$\int_0^\infty \frac{c_2 t}{\lambda^2} e^{-\frac{c_2 t^2}{2\lambda^2}} \mathbf{1}_{[\|x - P_{\mathcal{K}}(x)\|_2, +\infty)}(t) dt = e^{-\frac{c_2}{2\lambda^2}\|x - P_{\mathcal{K}}(x)\|_2^2},$$

it holds for every $k \geq 0$ that

$$\int_{\mathcal{K}^c} \|x\|_2^k e^{-f(x) - \frac{1}{2\lambda^2} d_{\mathcal{K}}(x)} dx \geq e^{-f(0)} \underbrace{\left(\int_{\mathcal{K}^c} \|x\|_2^k e^{-\frac{M}{2}\|x\|_2^2} \mathbf{1}_{[\|x - P_{\mathcal{K}}(x)\|_2, +\infty)}(t) dx \right)}_{\psi(t)} \frac{c_2 t}{\lambda^2} e^{-\frac{c_2 t^2}{2\lambda^2}} dt.$$

By Assumption 3, $\|x - P_{\mathcal{K}}(x)\|_2 \leq c_1^{-1/2} d_{\mathcal{K}}(x)^{1/2}$, therefore

$$\psi(t) \geq \int_{\mathcal{K}^c} \|x\|_2^k e^{-\frac{M}{2}\|x\|_2^2} \mathbf{1}(d_{\mathcal{K}}(x) \leq c_1 t^2) dx.$$

Define the set $\tilde{\mathcal{K}}_t := \{x \in \mathbb{R}^p : d_{\mathcal{K}}(x) \leq c_1 t^2\}$. Since $d_{\mathcal{K}}$ is M_0 -smooth, then it holds for any $x \in \mathcal{K}$ that

$$d_{\mathcal{K}}((1+b)x) \leq d_{\mathcal{K}}(x) + \langle \nabla d_{\mathcal{K}}(x), bx \rangle + M_0 \|bx\|_2^2 = M_0 b^2 \|x\|_2^2.$$

Let $b = \sqrt{c_1/M_0} t/R$, then $d_{\mathcal{K}}((1+b)x) \leq c_1 t^2$, it implies that $(1+b)\mathcal{K} \subseteq \tilde{\mathcal{K}}_t$. We then obtain that

$$\begin{aligned} \psi(t) &= \int_{\tilde{\mathcal{K}}_t} \|x\|_2^k e^{-\frac{M}{2}\|x\|_2^2} dx - \int_{\mathcal{K}} \|x\|_2^k e^{-\frac{M}{2}\|x\|_2^2} dx \\ &\geq \int_{(1+b)\mathcal{K}} \|x\|_2^k e^{-\frac{M}{2}\|x\|_2^2} dx - \int_{\mathcal{K}} \|x\|_2^k e^{-\frac{M}{2}\|x\|_2^2} dx \\ &= \int_{(1+b)\mathcal{K} - \mathcal{K}} \|x\|_2^k e^{-\frac{M}{2}\|x\|_2^2} dx. \end{aligned}$$

Denote the right side of the last equality by $\psi_1(t)$, then $\psi(t) \geq \psi_1(t)$, we have

$$\begin{aligned} \int_{\mathcal{K}^c} \|x\|_2^k e^{-f(x) - \frac{1}{2\lambda^2} d_{\mathcal{K}}(x)} dx &\geq e^{-f(0)} \int_0^\infty \psi_1(t) \frac{c_2 t}{\lambda^2} e^{-\frac{c_2 t^2}{2\lambda^2}} dt \\ &= e^{-f(0)} \int_0^\infty \psi_1(t) d\left(-e^{-c_2 t^2/2\lambda^2}\right) dt \\ &= e^{-f(0)} \int_0^\infty \psi'_1(t) e^{-\frac{c_2 t^2}{2\lambda^2}} dt. \end{aligned}$$

To compute $\psi'_1(t)$, we apply the Reynolds Transport Theorem to the t-dependent domain $(1 + b(t))\mathcal{K} - \mathcal{K}$, where $b(t) = \frac{\sqrt{c_1/M_0}}{R}t$. Parametrize the outer boundary $\partial[(1 + b(t))\mathcal{K}]$ by $x = (1 + b(t))y$ with $y \in \partial\mathcal{K}$. The outward normal velocity of the moving boundary is $v_{\vec{n}}(x) = \frac{db(t)}{dt} \cdot \|\nabla\gamma_{\mathcal{K}}(x)\|_2^{-1}$. By the theorem, the derivative becomes a boundary integral over $\partial[(1 + b(t))\mathcal{K}]$:

$$\psi'_1(t) = \int_{\partial[(1+b(t))\mathcal{K}]} \|x\|_2^k e^{-\frac{M}{2}\|x\|_2^2} v_{\vec{n}}(x) dS(x).$$

Substitute $x = (1 + b)y$ and $dS(x) = (1 + b)^{p-1}dS(y)$, we obtain

$$\begin{aligned} \psi'_1(t) &= \frac{\sqrt{c_1/M_0}}{R} (1 + b(t))^{k+p-1} \int_{\partial\mathcal{K}} \frac{\|y\|_2^k}{\|\nabla\gamma_{\mathcal{K}}(y)\|_2} e^{-\frac{M}{2}(1+b)^2\|y\|_2^2} dS(y) \\ &\geq \frac{\sqrt{c_1/M_0}r^{k+2}\mathcal{H}_{p-1}(\partial\mathcal{K})}{R} (1 + b(t))^{k+p-1} e^{-\frac{MR^2}{2}(1+b)^2} \\ &\geq C(c_1, M_0, \mathcal{K}) r^{p+k+1} e^{-\frac{MR^2}{2}(1+b)^2}. \end{aligned}$$

where the constant $C(c_1, M_0, \mathcal{K})$ is independent of r, p and k . Therefore, it follows that

$$\begin{aligned} \int_{\mathcal{K}^c} \|x\|_2^k e^{-f(x) - \frac{1}{2\lambda^2}d_{\mathcal{K}}(x)} dx &\geq C(c_1, M_0, \mathcal{K}) r^{p+k+1} \int_0^\infty e^{-\frac{c_2 t^2}{2\lambda^2} - \frac{MR^2}{2}(1+at)^2} dt \\ &\geq \tilde{C}(c_1, c_2, M_0, M, \mathcal{K}) r^{p+k-1} \lambda. \end{aligned}$$

where $a = \frac{\sqrt{c_1/M_0}}{R}$. Moreover, by Lemma 7, we find

$$\begin{aligned} \int_{\mathbb{R}^p} e^{-U^\lambda(x)} dx &= \int_{\mathcal{K}} e^{-U^\lambda(x)} dx + \int_{\mathcal{K}^c} e^{-U^\lambda(x)} dx \\ &\leq \left(1 + \frac{3\sqrt{\pi}p\lambda}{rc_1^{1/2}}\right) \mu_0(\nu). \end{aligned}$$

Furthermore, using the integration in polar coordinates gives

$$\int_{\mathcal{K}} \|x\|_2^k e^{-f(x)} dx \leq \omega_{p-1} \int_0^R t^{k+p-1} dt = \omega_{p-1} \frac{R^{k+p}}{k+p}$$

Collecting pieces and plugging into display (B.5)

$$\int_{\mathcal{K}^c} \|x\|_2^k \nu^\lambda(dx) / \mu_k(\nu) \geq \frac{\tilde{C}(c_1, c_2, M_0, M, \mathcal{K}) r^{p+k-1}(k+p)}{(1 + 3\sqrt{\pi}p\lambda/rc_1^{1/2})\omega_{p-1} R^{k+p}} \lambda.$$

□

C Proofs of Section 2.3 and Section 2.4

Condition C.1. *The function $U^\lambda(x)$ is m -strongly convex, continuously differentiable and M^λ -smooth. Moreover, it holds that $\int_{\mathbb{R}^p} e^{-U^\lambda(x)} dx < \infty$.*

Lemma 12. *Assume Assumptions 1- 4 hold, then the potential $U^{B,\lambda}$ satisfies Condition C.1 with $M^\lambda = \lambda_{\max}(Q)/\lambda^2 + M$.*

Proof. [Proof of Lemma 12] We factorize the matrix Q^{-1} as $Q^{-1} = DD^\top$. Define the composition operator $\ell_K \circ D(x) = \ell_K(Dx)$. It then follows that

$$\begin{aligned}\ell_K^{M,\lambda}(x) &= \inf_{y \in \mathbb{R}^p} \left(\ell_K(y) + \frac{1}{2\lambda^2} (x - y)^\top Q(x - y) \right) \\ &= \inf_{y \in \mathbb{R}^p} \left(\ell_K \circ D(y) + \frac{1}{2\lambda^2} (D^{-1}x - y)^\top D^\top Q D (D^{-1}x - y) \right) \\ &= \inf_{y \in \mathbb{R}^p} \left(\ell_K \circ D(y) + \frac{1}{2\lambda^2} \|D^{-1}x - y\|_2^2 \right).\end{aligned}$$

Define $e_\lambda(\ell_K \circ D)(x) := \ell_K^{M,\lambda} \circ D(x)$, then

$$e_\lambda(\ell_K \circ D)(x) = \inf_{y \in \mathbb{R}^p} \left(\ell_K \circ D(y) + \frac{1}{2\lambda^2} \|x - y\|_2^2 \right)$$

is a Moreau envelope function of the composite function $\ell_K \circ D$, and the corresponding proximal mapping is

$$P_\lambda(\ell_K \circ D)(x) := \operatorname{argmin}_{y \in D^{-1}K} \left(\ell_K \circ D(y) + \frac{1}{2\lambda^2} \|x - y\|_2^2 \right).$$

By Theorem 2.26 in [RW09], the envelope function $e_\lambda(\ell_K \circ D)$ is convex, continuously differentiable, and its gradient is as follows

$$\nabla e_\lambda(\ell_K \circ D)(x) = \frac{1}{\lambda^2} (x - P_\lambda(\ell_K \circ D)(x)).$$

Note that $\ell_K \circ D$ is convex, then $P_\lambda(\ell_K \circ D)$ is maximal monotone and nonexpansive. By Proposition 12.19 in [RW09], we have

$$\|\nabla e_\lambda(\ell_K \circ D)(x_1) - \nabla e_\lambda(\ell_K \circ D)(x_2)\|_2 \leq \frac{1}{\lambda^2} \|x_1 - x_2\|_2.$$

Recall that $e_\lambda(\ell_K \circ D)(x) = \ell_K^{M,\lambda} \circ D(x)$, it then follows that

$$\begin{aligned}\|\nabla \ell_K^{M,\lambda}(x_1) - \nabla \ell_K^{M,\lambda}(x_2)\|_2 &= \|D^{-\top} \nabla (\ell_K^{M,\lambda} \circ D)(D^{-1}x_1) - D^{-\top} \nabla (\ell_K^{M,\lambda} \circ D)(D^{-1}x_2)\|_2 \\ &= \|D^{-\top} \nabla e_\lambda(\ell_K \circ D)(D^{-1}x_1) - D^{-\top} \nabla e_\lambda(\ell_K \circ D)(D^{-1}x_2)\|_2 \\ &\leq \frac{1}{\lambda^2} \|D^{-1}\|_2 \|D^{-1}x_1 - D^{-1}x_2\|_2 \\ &\leq \frac{1}{\lambda^2} \|D^{-1}\|_2^2 \|x_1 - x_2\|_2.\end{aligned}$$

Since $Q^{-1} = DD^\top$, it holds that $\|D^{-1}\|_2^2 = \lambda_{\max}(Q)$. Therefore, we obtain

$$M^\lambda = M + \frac{\lambda_{\max}(Q)}{\lambda^2}.$$

Now we show that $\int_{\mathbb{R}^p} e^{-U^{M,\lambda}(s)} ds < \infty$. Note that

$$\int_{\mathbb{R}^p} e^{-U^{M,\lambda}(x)} dx = \int_{\mathcal{K}} e^{-f(x)} dx + \int_{\mathcal{B}_2(0,R) \cap \mathcal{K}^c} e^{-U^{M,\lambda}(x)} dx + \int_{\mathcal{B}_2(0,R)^c} e^{-U^{M,\lambda}(x)} dx.$$

We now derive the bound for the second and the third terms on the right-hand side of the previous display. Since $f \geq l$, we then find

$$\int_{\mathcal{B}_2(0,R) \cap \mathcal{K}^c} e^{-U^{M,\lambda}(x)} dx \leq e^{-l} \int_{\mathcal{B}_2(0,R)} dx.$$

Thus,

$$\int_{\mathcal{B}_2(0,R) \cap \mathcal{K}^c} e^{-U^{M,\lambda}(x)} dx \leq e^{-l} \int_{\mathcal{B}_2(0,R)} dx = e^{-l} \frac{\pi^{p/2}}{\Gamma(\frac{d}{2} + 1)} R^p < \infty.$$

It remains to show $\int_{\mathbb{R}^p} e^{-U^{M,\lambda}(s)} ds < \infty$.

$$\begin{aligned} \int_{\mathcal{B}_2(0,R)^c} e^{-U^{M,\lambda}(x)} dx &= \int_{\mathcal{B}_2(0,R)^c} e^{-f(x)} \exp\left(-\inf_{x' \in D^{-1}\mathcal{K}} \frac{1}{2\lambda^2} \|D^{-1}x - x'\|_2^2\right) dx \\ &\leq e^{-l} \int_{\mathcal{B}_2(0,R)^c} \exp\left(-\inf_{x' \in \mathcal{K}} \frac{1}{\lambda^2 \|D\|_2^2} \|x - x'\|_2^2\right) dx \\ &\leq e^{-l} \int_{\mathcal{B}_2(0,R)^c} \exp\left(-\frac{1}{\lambda^2 \|Q^{-1}\|_2} (\|x\|_2 - R)^2\right). \end{aligned}$$

By Fubini's theorem and the fact that

$$e^{-\frac{1}{\alpha}(\|x\|_2 - R)^2} = \int_0^\infty \frac{2t}{\alpha} e^{-\frac{t^2}{\alpha}} \mathbf{1}_{[\|x\|_2 - R, \infty)}(t) dt,$$

we obtain

$$\begin{aligned} \int_{\mathcal{B}_2(0,R)^c} e^{-U^{M,\lambda}(x)} dx &\leq e^{-l} \int_0^\infty \frac{2t}{\lambda^2 \|Q^{-1}\|_2} e^{-\frac{t}{\lambda^2 \|Q^{-1}\|_2}} \int_{x: \|x\|_2 \geq R} \mathbf{1}_{[\|x\|_2 - R, \infty)}(t) dx dt \\ &\leq e^{-l} \int_0^\infty \frac{2t}{\lambda^2 \|Q^{-1}\|_2} e^{-\frac{t}{\lambda^2 \|Q^{-1}\|_2}} \int_{\mathcal{B}_2(0,R+t)} dx dt \\ &= e^{-l} \int_0^\infty \frac{2t}{\lambda^2 \|Q^{-1}\|_2} e^{-\frac{t}{\lambda^2 \|Q^{-1}\|_2}} \frac{\pi^{p/2}}{\Gamma(\frac{p}{2} + 1)} (R + t)^d dt \\ &< \infty. \end{aligned}$$

Collecting pieces gives the desired result. \square

Lemma 13. *Assume Assumptions 1-4 hold, then the surrogate potential $U^{G,\lambda}$ satisfies Condition C.1 with $M^\lambda = (1 + C_{\mathcal{K}}r)/\lambda^2 + M$, where $C_{\mathcal{K}}$ is a constant dependent on \mathcal{K} .*

Proof. [Proof of Lemma 13]

Convex. Since \mathcal{K} is convex, the Gauge function of set \mathcal{K} is then convex, note that $h(u) = (u - 1)^2$ is convex and non-decreasing on $[1, \infty)$, therefore the composition of h and $g_{\mathcal{K}}$ is convex, which is $d_{\mathcal{K}}$.

Smooth. Denote the original Gauge function by $\gamma_K(x) := \inf\{t \geq 0 : x \in t\mathcal{K}\}$, therefore $g_K = 1$ inside \mathcal{K} and $g_K(x) = \gamma_K(x)$ outside \mathcal{K} . For $d_K(x) = (g_K(x) - 1)^2$, we analyze its smoothness outside \mathcal{K} . In \mathcal{K}^c , the Hessian matrix is

$$H_{d_K} = 2\nabla g_K(\nabla g_K)^\top + 2(g_K - 1)H_{g_K},$$

where $H_{g_K} = H_{\gamma_K}$ since $g_K = \gamma_K$ in this region, therefore $\|\nabla g_K(x)\|_2 = \|\nabla \gamma_K(x)\|_2$. For any direction $h \in \mathbb{R}^p$, the directional derivative satisfies $\gamma_K(x + h) - \gamma_K(x) \geq \nabla \gamma_K(x) \cdot h$ by convexity of γ_K . Simultaneously, sublinearity implies $\gamma_K(x + h) \leq \gamma_K(x) + \gamma_K(h)$. Combining these we have $\nabla \gamma_K(x) \cdot h \leq \gamma_K(h)$. Choose $h = \nabla \gamma_K(x)/\|\nabla \gamma_K(x)\|_2$, it then holds that $\|\nabla \gamma_K(x)\|_2 \leq \gamma_K(h) \leq \frac{1}{r}$. The first term $2\nabla g_K(\nabla g_K)^\top$ is rank-1, with its spectral norm bounded by $2\|\nabla \gamma_K\|^2 \leq 2/r^2$. For the second term, on the unit sphere \mathbb{S}^{p-1} , the continuity of H_{γ_K} over the compact \mathcal{K} ensures a finite maximum eigenvalue C_K , where C_K only depends on \mathcal{K} . By 1-homogeneity of γ_K , we have $H_{\gamma_K}(tx) = \frac{1}{t}H_{\gamma_K}(x)$, it implies

$$\|H_{g_K}(x)\|_2 = \|H_{\gamma_K}(x)\|_2 \leq \frac{C_K}{\|x\|_2}.$$

We also have $g_K(x) \leq \|x\|_2/r$. Combining these, the eigenvalues of H_{d_K} in \mathcal{K}^c are uniformly bounded by $2/r^2 + 2C_K/r$. Consequently, d_K is $\frac{2(1+C_Kr)}{r^2}$ -smooth in \mathcal{K}^c , and $d_K \equiv 0$ implies 0-smoothness in \mathcal{K} . For the global smoothness over \mathbb{R}^p , observe that for any $x \in \mathcal{K}$ and $y \in \mathcal{K}^c$, let z be the intersection of $\partial\mathcal{K}$ with line segment \vec{xy} , $\|\nabla d_K(y) - \nabla d_K(x)\|_2 = \|\nabla d_K(y)\|_2 = \|\nabla d_K(y) - \nabla d_K(z)\|_2$ by the fact that $\nabla d_K|_{\partial\mathcal{K}} \equiv 0$, then

$$\|\nabla d_K(y) - \nabla d_K(x)\|_2 = \|\nabla d_K(y) - \nabla d_K(z)\|_2 \leq \frac{2(1+C_Kr)}{r^2}\|y - z\|_2 \leq \frac{2(1+C_Kr)}{r^2}\|y - x\|_2$$

Thus, d_K is globally $\frac{2(1+C_Kr)}{r^2}$ -smooth.

To show that $\int_{\mathbb{R}^p} e^{-U^{G,\lambda}(x)} dx < \infty$. Note that

$$\int_{\mathbb{R}^p} e^{-U^{G,\lambda}(x)} dx = \int_{\mathcal{K}} e^{-f(x)} dx + \int_{\mathcal{B}_2(0,R) \cap \mathcal{K}^c} e^{-U^{G,\lambda}(x)} dx + \int_{\mathcal{B}_2(0,R)^c} e^{-U^{G,\lambda}(x)} dx.$$

The first term and the second term have the same bound as in the proof of Lemma 12, since we only need the property that $\ell_K^{G,\lambda} \geq 0$. For the third term, similarly, by Fubini's theorem and the fact that

$$e^{-\frac{1}{2\lambda^2}(g_K(x)-1)^2} = \int_0^\infty \frac{t}{\lambda^2} e^{-\frac{t^2}{2\lambda^2}} \mathbb{1}_{[g_K(x)-1,\infty)}(t) dt,$$

we obtain

$$\begin{aligned} \int_{\mathcal{B}_2(0,R)^c} e^{-U^{G,\lambda}(x)} dx &\leq e^{-l} \int_0^\infty \frac{t}{\lambda^2} e^{-\frac{t}{2\lambda^2}} \int_{x: \|x\|_2 \geq R} \mathbb{1}_{[g_K(x)-1,\infty)}(t) dx dt \\ &\leq e^{-l} \int_0^\infty \frac{t}{\lambda^2} e^{-\frac{t}{2\lambda^2}} \int_{\mathcal{B}_2(0,(1+t)R)} dx dt \\ &= e^{-l} \int_0^\infty \frac{t}{\lambda^2} e^{-\frac{t}{2\lambda^2}} \frac{\pi^{p/2}}{\Gamma(p/2+1)} ((1+t)R)^p dt \\ &= \frac{e^{-l}\pi^{p/2}R^p}{\Gamma(p/2+1)} \int_0^\infty s e^{-s^2/2} (1+\lambda s)^p ds \\ &< \infty. \end{aligned}$$

Then we reach the desired result. \square

C.1 Proof of Theorem 3

Proposition 14. Set $M^\lambda = M + M_0/\lambda^2$, $\kappa = M^\lambda/m$, choose the initial point to be the minimizer of the function f , then we have

$$W_2(\nu_n^{\text{CRLMC}}, \nu) \leq 1.1e^{-\frac{mnh}{2}} W_2(\nu_0^{\text{CRLMC}}, \nu) + (2.4\sqrt{\kappa M^\lambda h} + 1.77) M^\lambda h \sqrt{p/m} + 2.1 W_2(\nu^\lambda, \nu)$$

and

$$W_1(\nu_n^{\text{CRLMC}}, \nu) \leq 1.1e^{-\frac{mnh}{2}} (2R + 1 + \sqrt{p/m}) + (2.4\sqrt{\kappa M^\lambda h} + 1.77) M^\lambda h \sqrt{p/m} + W_1(\nu^\lambda, \nu).$$

Proof. The triangle inequality for the Wasserstein distance provides us with

$$W_2(\nu_n^{\text{CRLMC}}, \nu) \leq W_2(\nu_n^{\text{CRLMC}}, \nu^\lambda) + W_2(\nu^\lambda, \nu). \quad (\text{C.1})$$

By Theorem 1 in [YKD23], it holds that

$$W_2(\nu_n^{\text{CRLMC}}, \nu^\lambda) \leq 1.1e^{-\frac{mnh}{2}} W_2(\nu_0^{\text{CRLMC}}, \nu^\lambda) + (2.4\sqrt{\kappa M^\lambda h} + 1.77) M^\lambda h \sqrt{p/m} \quad (\text{C.2})$$

provided that $M^\lambda h + \sqrt{\kappa}(M^\lambda h)^{3/2} \leq 1/4$. Using the triangle inequality for the Wasserstein distance again gives

$$W_2(\nu_n^{\text{CRLMC}}, \nu) \leq 1.1e^{-\frac{mnh}{2}} W_2(\nu_0^{\text{CRLMC}}, \nu) + (2.4\sqrt{\kappa M^\lambda h} + 1.77) M^\lambda h \sqrt{p/m} + 2.1 W_2(\nu^\lambda, \nu)$$

When ν_0^{CRLMC} is the Dirac mass at the minimizer of the function f , by Proposition 1 in [DM19], it holds that

$$W_2(\nu_0^{\text{CRLMC}}, \nu) \leq \sqrt{\frac{p}{m}}.$$

Plugging this back to display (C.1) then provides us with

$$W_2(\nu_n^{\text{CRLMC}}, \nu) \leq 1.1e^{-\frac{mnh}{2}} \sqrt{\frac{p}{m}} + (2.4\sqrt{\kappa M^\lambda h} + 1.77) M^\lambda h \sqrt{p/m} + 2.1 W_2(\nu, \nu^\lambda).$$

This completes the proof of the first claim.

We then proceed to prove the second claim. By the triangle inequality and the monotonicity of Wasserstein distance, we have

$$\begin{aligned} W_1(\nu_n^{\text{CRLMC}}, \nu) &\leq W_1(\nu_n^{\text{CRLMC}}, \nu^\lambda) + W_1(\nu^\lambda, \nu) \\ &\leq W_2(\nu_n^{\text{CRLMC}}, \nu^\lambda) + W_1(\nu^\lambda, \nu). \end{aligned}$$

When ν_0^{CRLMC} is the Dirac mass at the minimizer x_0 of the function f , denote the minimizer of the function U^λ by x^* , by Proposition 1 in [DM19], it holds that

$$W_2(\nu_0^{\text{CRLMC}}, \nu^\lambda) \leq W_2(\nu_0^{\text{CRLMC}}, \delta_{x_*}) + W_2(\delta_{x_*}, \nu^\lambda) \leq \|x_0 - x^*\|_2 + \sqrt{p/m}.$$

Since

$$u \geq U^\lambda(x_0) = f(x_0) + \frac{1}{2\lambda^2} d_K(x_0) \geq l + \frac{c_1}{2\lambda^2} \|x_0 - P_K(x_0)\|_2^2,$$

we have

$$\|x_0 - x^*\|_2 \leq \|x_0 - P_{\mathcal{K}}(x_0)\|_2 + \|P_{\mathcal{K}}(x_0) - x^*\|_2 \leq 2R + \sqrt{2(u-l)/c_1}\lambda < 2R + 1.$$

Combining this with previous display, display (C.2), and Proposition 1 then gives

$$\begin{aligned} W_1(\nu_n^{\text{CRLMC}}, \nu) &\leq 1.1e^{-\frac{mnh}{2}} W_2(\nu_0^{\text{CRLMC}}, \nu^\lambda) + (2.4\sqrt{\kappa M^\lambda h} + 1.77)M^\lambda h \sqrt{p/m} + W_1(\nu^\lambda, \nu) \\ &\leq 1.1e^{-\frac{mnh}{2}} (2R + 1 + \sqrt{p/m}) + (2.4\sqrt{\kappa M^\lambda h} + 1.77)M^\lambda h \sqrt{p/m} + W_1(\nu^\lambda, \nu). \end{aligned}$$

as desired. \square

Proof. [Proof of Theorem 3] Combining Proposition 1 with Proposition 14, we have

$$W_2(\nu_n^{\text{CRLMC}}, \nu) \leq 1.1e^{-\frac{mnh}{2}} \sqrt{p/m} + (2.4\sqrt{\kappa M^\lambda h} + 1.77)M^\lambda h \sqrt{p/m} + 2.1C(p, 2)\lambda^{\frac{1}{2}+\frac{1}{p}}$$

To reach the best convergence rate, we choose

$$\lambda = \left(\frac{19.2M_0^2}{2.1m} \right)^{\frac{2p}{9p+2}} \frac{p^{3p/(9p+2)}}{(C(p, 2)(p+2))^{2p/(9p+2)}} h^{\frac{3p}{9p+2}}.$$

Substitute λ into the upper bound, then it is enough to choose

$$h \leq A_1 \varepsilon^{\frac{18p+4}{3p+6}} \frac{p^{8p/(3p+6)}}{C(p, 2)^{16p/(3p+6)}} M_0^{-\frac{4}{3}} m^{-\frac{7p-2}{3p+6}}$$

where $A_1 = [3 \times (2.1 \times (9.6/2.1)^{(p+2)/(9p+2)} + 2.4 \times (19.2/2.1)^{-8p/(9p+2)})]^{-(18p+4)/(3p+6)}$. Then

$$n \geq \frac{2}{mh} \ln \left(\frac{3.3}{\varepsilon} \right).$$

Similarly, for $q = 1$, we have

$$W_1(\nu_n^{\text{CRLMC}}, \nu) \leq 1.1e^{-\frac{mnh}{2}} (2R + 1 + \sqrt{p/m}) + (2.4\sqrt{\kappa M^\lambda h} + 1.77)M^\lambda h \sqrt{p/m} + C(p, 1)\lambda.$$

Then the optimal λ is

$$\lambda = 9.6^{1/5} p^{1/10} C(p, 1)^{-1/5} M_0^{2/5} m^{-1/5} h^{3/10}.$$

Therefore we choose

$$h \leq 0.0027 \varepsilon^{\frac{10}{3}} \frac{p^{4/3}}{C(p, 1)^{8/3}} M_0^{-\frac{4}{3}} m^{-1},$$

and

$$n \geq \frac{2}{mh} \ln \left(\frac{3.3(2R + 1 + \sqrt{p/m})}{\varepsilon \sqrt{p/m}} \right)$$

\square

C.2 Proof of Theorem 4

Proposition 15. Choose γ and h so that $\gamma \geq 5M^\lambda$ and $\gamma h \leq 0.1\kappa^{-1/6}$, where $\kappa = M^\lambda/m$. Assume that the initial point ϑ_0 is the minimizer of the function f , and that $\mathbf{v}_0 \sim \mathcal{N}_p(0, \gamma \mathbf{I}_p)$. Then

$$W_2(\nu_n^{\text{CRKLMC}}, \nu) \leq 1.6e^{-mn} \sqrt{p/m} + 0.2(\gamma h)^3 \sqrt{\kappa p/m} + 10(\gamma h)^{3/2} \sqrt{p/m} + 2.6W_2(\nu^\lambda, \nu).$$

and

$$W_1(\nu_n^{\text{CRKLMC}}, \nu) \leq 1.6e^{-mn} (2R + 1 + \sqrt{p/m}) + 0.2(\gamma h)^3 \sqrt{\kappa p/m} + 10(\gamma h)^{3/2} \sqrt{p/m} + W_1(\nu^\lambda, \nu).$$

Proof. The proof employs a similar technique to that used in the proof of Theorem 3. By the triangle inequality and Theorem 2 from [YKD23], we have

$$\begin{aligned} W_2(\nu_n^{\text{CRKLMC}}, \nu) &\leq W_2(\nu^\lambda, \nu) + W_2(\nu_n^{\text{CRKLMC}}, \nu^\lambda) \\ &\leq 1.6e^{-mn} W_2(\nu_0^{\text{CRKLMC}}, \nu^\lambda) + 0.2(\gamma h)^3 \sqrt{\kappa p/m} + 10(\gamma h)^{3/2} \sqrt{p/m} + W_2(\nu^\lambda, \nu) \\ &\leq 1.6e^{-mn} W_2(\nu_0^{\text{CRKLMC}}, \nu) + 0.2(\gamma h)^3 \sqrt{\kappa p/m} + 10(\gamma h)^{3/2} \sqrt{p/m} + 2.6W_2(\nu^\lambda, \nu). \end{aligned}$$

Since ν_0^{CRKLMC} is the minimizer of f , then we have

$$\begin{aligned} W_2(\nu_n^{\text{CRKLMC}}, \nu) &\leq W_2(\nu^\lambda, \nu) + W_2(\nu_n^{\text{CRKLMC}}, \nu^\lambda) \\ &\leq 1.6e^{-mn} \sqrt{p/m} + 0.2(\gamma h)^3 \sqrt{\kappa p/m} + 10(\gamma h)^{3/2} \sqrt{p/m} + 2.6W_2(\nu^\lambda, \nu). \end{aligned}$$

For the second claim, it holds that

$$\begin{aligned} W_1(\nu_n^{\text{CRKLMC}}, \nu) &\leq W_2(\nu^\lambda, \nu) + W_1(\nu_n^{\text{CRKLMC}}, \nu^\lambda) \\ &\leq 1.6e^{-mn} W_2(\nu_0^{\text{CRKLMC}}, \nu^\lambda) + 0.2(\gamma h)^3 \sqrt{\kappa p/m} + 10(\gamma h)^{3/2} \sqrt{p/m} + W_1(\nu^\lambda, \nu) \\ &\leq 1.6e^{-mn} (2R + 1 + \sqrt{p/m}) + 0.2(\gamma h)^3 \sqrt{\kappa p/m} + 10(\gamma h)^{3/2} \sqrt{p/m} + W_1(\nu^\lambda, \nu). \end{aligned}$$

□

Proof. [Proof of Theorem 4] Combining Proposition 15 with Proposition 1, we have

$$W_2(\nu_n^{\text{CRKLMC}}, \nu) \leq 1.6e^{-mn} \sqrt{p/m} + 0.2(\gamma h)^3 \sqrt{\kappa p/m} + 10(\gamma h)^{3/2} \sqrt{p/m} + 2.6C(p)\lambda^{\frac{1}{2}+\frac{1}{p}}.$$

$$\lambda = \left(\frac{150M_0^{7/2}}{m} \right)^{\frac{2p}{15p+2}} \frac{p^{p/(15p+2)}}{C(p, 2)^{2p/(15p+2)}} h^{\frac{6p}{15p+2}}.$$

$$h \leq A_2 \varepsilon^{\frac{15p+2}{3p+6}} \frac{p^{7p/(3p+6)}}{C(p, 2)^{14p/(3p+6)}} M_0^{-\frac{7}{6}} m^{-\frac{13p-2}{6p+12}}$$

where $A_2 = [3 \times (25 \times 150^{-14p/(15p+2)} + 2.6 \times 75^{(p+2)/(15p+2)})]^{-(15p+2)/(3p+6)}$.

$$n \geq \frac{1}{mh} \ln \left(\frac{4.8}{\varepsilon} \right)$$

Similarly, for $q = 1$, we have

$$W_1(\nu_n^{\text{CRKLMC}}, \nu) \leq 1.6e^{-mn} (2R + 1 + \sqrt{p/m}) + 0.2(\gamma h)^3 \sqrt{\kappa p/m} + 10(\gamma h)^{3/2} \sqrt{p/m} + C(p, 1)\lambda.$$

Then the optimal λ is

$$\lambda = 1.91 h^{3/8} p^{1/16} C(p, 1)^{-1/8} M_0^{7/16} m^{-1/8}.$$

Thus we choose

$$h \leq 0.0067 \varepsilon^{\frac{8}{3}} \frac{p^{7/6}}{C(p, 1)^{7/3}} M_0^{-7/6} m^{-1},$$

and

$$n \geq \frac{1}{nh} \ln \left(\frac{4.8(2R + 1 + \sqrt{p/m})}{\varepsilon \sqrt{p/m}} \right).$$

□

D Proofs of Section 2.5

D.1 Proof of Theorem 5

Proposition 16. *Let the step size $h \in (0, 1/M^\lambda)$ and $\lambda = o(r/p)$. The initial distribution ν_0^{CLMC} is set to be the Dirac measure at the minimizer of f , then it holds that*

$$W_2(\nu_n^{\text{CLMC}}, \nu) \leq e^{-\frac{mnh}{2}} \sqrt{p/m} + \sqrt{\frac{2M^\lambda ph}{m}} + 2W_2(\nu^\lambda, \nu),$$

and

$$W_1(\nu_n^{\text{CLMC}}, \nu) \leq e^{-\frac{mnh}{2}} (2R + 1 + \sqrt{p/m}) + \sqrt{\frac{2M^\lambda ph}{m}} + W_1(\nu^\lambda, \nu).$$

Proof. By Theorem 9 in [DMM19] and the triangle inequality for the Wasserstein distance, it holds that

$$\begin{aligned} W_2(\nu_n^{\text{CLMC}}, \nu) &\leq W_2(\nu_n^{\text{CLMC}}, \nu^\lambda) + W_2(\nu^\lambda, \nu) \\ &\leq e^{-\frac{mnh}{2}} W_2(\nu_0^{\text{CLMC}}, \nu^\lambda) + \sqrt{\frac{2M^\lambda ph}{m}} + W_2(\nu^\lambda, \nu) \end{aligned}$$

provided that $h \leq 1/M^\lambda$. Since ν_0^{CLMC} is the Dirac mass at the minimizer of the function f , by the triangle inequality and Proposition 1 in [DM19], it holds that

$$\begin{aligned} W_2(\nu_n^{\text{CLMC}}, \nu) &\leq e^{-\frac{mnh}{2}} W_2(\nu_0^{\text{CLMC}}, \nu) + \sqrt{\frac{2M^\lambda ph}{m}} + 2W_2(\nu^\lambda, \nu) \\ &\leq e^{-\frac{mnh}{2}} \sqrt{p/m} + \sqrt{\frac{2M^\lambda ph}{m}} + 2W_2(\nu^\lambda, \nu). \end{aligned}$$

For $q = 1$, we have

$$W_1(\nu_n^{\text{CLMC}}, \nu) \leq e^{-\frac{mnh}{2}} (2R + 1 + \sqrt{p/m}) + \sqrt{\frac{2M^\lambda ph}{m}} + W_1(\nu^\lambda, \nu)$$

as desired. \square

Proof. [Proof of Theorem 5] By Proposition 16, we have

$$W_2(\nu_n^{\text{CLMC}}, \nu) \leq e^{-\frac{mnh}{2}} \sqrt{p/m} + \sqrt{\frac{2M^\lambda ph}{m}} + 2W_2(\nu^\lambda, \nu).$$

Using Proposition 1, it holds that

$$W_2(\nu_n^{\text{CLMC}}, \nu) \leq e^{-\frac{mnh}{2}} \sqrt{p/m} + \sqrt{\frac{2M^\lambda ph}{m}} + 2C(p, 2)\lambda^{\frac{1}{2} + \frac{1}{p}}.$$

The optimal λ is

$$\lambda = \left(\frac{2M_0}{m} \right)^{\frac{p}{3p+2}} \frac{p^{3p/(3p+2)}}{(C(p, 2)(p+2))^{2p/(3p+2)}} h^{\frac{p}{3p+2}}$$

Then we choose

$$h \leq A_3 \varepsilon^{\frac{6p+4}{p+2}} \frac{p^{2p/(p+2)}}{C(p, 2)^{4p/(p+2)}} M_0^{-1} m^{-\frac{2p}{p+2}}$$

where $A_3 = [3 \times (2^{(p+2)/(6p+4)} + 2^{(5p+2)/(6p+4)})]^{-(6p+4)/(p+2)}$, and

$$n \geq \frac{2}{mh} \ln\left(\frac{3}{\varepsilon}\right)$$

For $q = 1$, we have

$$W_1(\nu_n^{\text{CLMC}}, \nu) \leq e^{-\frac{mnh}{2}} (2R + 1 + \sqrt{p/m}) + \sqrt{\frac{2M^\lambda ph}{m}} + C(p, 1)\lambda.$$

Then the optimal $\lambda = 1.19h^{1/4}p^{1/4}C(p, 1)^{-1/2}M_0^{1/4}m^{-1/4}$, thus we choose

$$h \leq 0.00039 \varepsilon^4 \frac{p}{C(p, 1)^2} M_0^{-1} m^{-1},$$

and

$$n \geq \frac{2}{mh} \ln\left(\frac{3(2R + 1 + \sqrt{p/m})}{\varepsilon \sqrt{p/m}}\right).$$

□

D.2 Proof of Theorem 6

Proposition 17. Choose γ and h so that $\gamma \geq 5M^\lambda$ and $\sqrt{\kappa}\gamma h \leq 0.1$, where $\kappa = M^\lambda/m$. Assume that ϑ_0 is the minimizer of f and $\mathbf{v}_0 \sim \mathcal{N}(0, \gamma\mathbf{I}_p)$, then it holds that

$$W_2(\nu_n^{\text{CKLMC}}, \nu) \leq 2e^{-mhn} \sqrt{p/m} + 0.9\gamma h \sqrt{\kappa p/m} + 3W_2(\nu^\lambda, \nu_0),$$

and

$$W_1(\nu_n^{\text{CKLMC}}, \nu) \leq 2e^{-mhn} (2R + 1 + \sqrt{p/m}) + 0.9\gamma h \sqrt{\kappa p/m} + W_1(\nu, \nu^\lambda).$$

Proof. By Theorem 3 from [YKD23], following the same approach in the proof of Proposition 14- 16, we arrive at the desired results. □

Proof. [Proof of Theorem 6] By Proposition 1, we have

$$W_2(\nu_n^{\text{CKLMC}}, \nu) \leq 2e^{-mhn} \sqrt{p/m} + 0.9\gamma h \sqrt{\kappa p/m} + 3C(p, 2)\lambda^{\frac{1}{2}+\frac{1}{p}},$$

Then the optimal λ is chosen to be

$$\lambda = \left(\frac{9M_0^{3/2}}{m}\right)^{\frac{2p}{7p+2}} \frac{p^{3p/(7p+2)}}{(C(p, 2)(p+2))^{2p/(7p+2)}} h^{\frac{2p}{7p+2}}$$

Thus it is enough to let

$$h \leq A_4 \varepsilon^{\frac{7p+2}{p+2}} \frac{p^{3p/(p+2)}}{C(p, 2)^{6p/(p+2)}} M_0^{-3/2} m^{-\frac{5p-2}{2p+4}},$$

and

$$n \geq \frac{1}{mh} \ln \left(\frac{6}{\varepsilon} \right).$$

For $q = 1$,

$$\mathbb{W}_1(\nu_n^{\text{CKLMC}}, \nu) \leq 2e^{-mhn}(2R + 1 + \sqrt{p/m}) + 0.9\gamma h \sqrt{\kappa p/m} + C(p, 1)\lambda.$$

The optimal $\lambda = 1.92h^{1/4}p^{1/8}C(p, 1)^{-1/4}M_0^{3/8}m^{-1/4}$

$$h \leq 0.00029\varepsilon^4 \frac{p^{3/2}}{C(p, 1)^3} M_0^{-3/2} m^{-1},$$

and

$$n \geq \frac{1}{mh} \ln \left(\frac{6(2R + 1 + \sqrt{p/m})}{\varepsilon \sqrt{p/m}} \right).$$

□

E Numerical Studies

Figures 3 and 4 show scatter plots of the four algorithms with $n = 2000$ and $N = 1000$. The red dashed lines indicate the boundaries of the constraint sets. These plots exhibit the same trends as those presented in the main text: CRKLMC demonstrates the best convergence, with samples most tightly concentrated within the constraint set. CRLMC outperforms CLMC, and CRKLMC improves upon CKLMC, illustrating the advantage of midpoint randomization over Euler discretization.

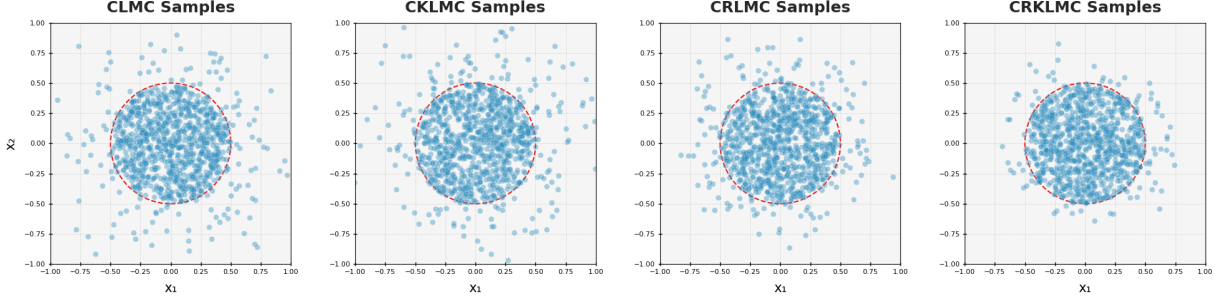


Figure 3: Scatter plots of samples generated by {CL,CKL,CRL,CRKL}MC algorithms.

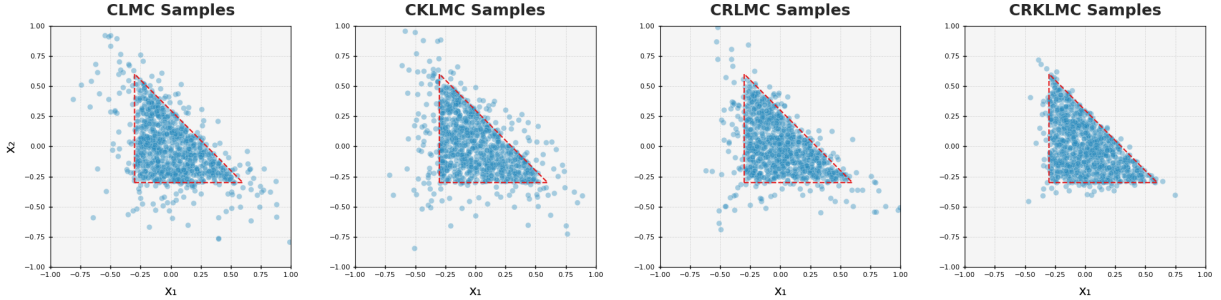


Figure 4: Scatter plots of samples generated by {CL,CKL,CRL,CRKL}MC algorithms.

The execution times for the algorithms are as follows,

Algorithm	$\mathcal{K} = \mathcal{B}_2(0.5)$		\mathcal{K} is 3-simplex	
	$n = 1000, N = 500$	$n = 2000, N = 1000$	$n = 1000, N = 500$	$n = 2000, N = 1000$
CLMC	11.95s	47.69s	10.73s	44.66s
CKLMC	35.52s	140.05s	32.64s	140.04s
CRLMC	24.60s	95.79s	22.73s	91.52s
CRKLMC	57.54s	221.60s	53.43s	213.88s